

Principal Structure Identification: Fast Disentanglement of Multi-source Dataset

SeoWon Choi*

Department of Statistics, Seoul National University
and

Sungkyu Jung

Department of Statistics, Seoul National University

March 29, 2022

Abstract

Analysis of multi-source data, where data on the same objects are collected from multiple sources, is of rising importance in many fields, e.g., multi-omics biology. Major challenges in multi-source data analysis include heterogeneity among different data sources and the entanglement of their association structure among several groups of variables. Our goal is to disentangle the association structure by identifying shared score subspaces among all or some of data blocks. We propose a sequential algorithm that gathers score subspaces of different data blocks within certain angle threshold and identifies partially-shared score components, using the concept of principal angles between subspaces of different dimensions. Our method shows better performance in identifying the linear association structure than competing methods in this field. In real data analysis, we apply our method to an oncological multi-omics dataset associated with drug responses. The proposed method boasts super-fast computational speed and results in revealing the scores in the estimated shared component showing strong correlations with well-known biological pathways. Supplementary materials for this article are available online.

Keywords: Correlation disentanglement; Data integration; Principal angles; Truncated singular value decomposition; Blood cancer multi-omics

*This work was supported by Samsung Science and Technology Foundation under Project Number SSTF-BA2002-03.

1 Introduction

In various fields of science and technology, there is a growing interest in analyzing multi-source data in an integrative way. By the multi-source data, we mean data measured for multiple groups of variables on the same set of subjects. Observations for each group of variables are obtained from a single source of experimental measurement and form a block of data matrix. A prominent example of multi-source data is modern multi-omics data that includes gene expressions, RNA sequencing, mutations, epigenetic markers or metagenomic materials (Subramanian et al., 2020). The recent development in high-throughput technique enables us to extract these sources of information comprehensively from a given preparation of cancer/normal tissue samples (Reuter et al., 2015; Norris et al., 2017).

In this paper, we propose a new method, called *Principal Structure Identification* (PSI), that disentangles the inherent association structure between groups of variables and integrates multiple datasets.

Consider a collection of K groups of variables. Each group of variables consists of p_k random variables and can be represented by a random vector $x_k \in \mathbb{R}^{p_k}$ for $k = 1, \dots, K$. The sizes of groups p_k are not necessarily the same. A random vector x_k is indeed a signal perturbed additively by a random error, that is, x_k is decomposed as $x_k = z_k + e_k \in \mathbb{R}^{p_k}$, where z_k is a random vector for signal and e_k for random noise. We impose a distributional assumption on e_k that it is an isotropic mean-zero random vector, as in Vershynin (2018). Without loss of generality, we give every variable in z_k zero mean and so in x_k subsequently.

We make an assumption on the relations among groups of variables, that is, some groups of variables share one or more latent variable. We name such variable groups, subsets of $\{1, \dots, K\}$, partial clusters. For given groups of variables $\{x_k\}_{k=1}^K$, there can exist multiple partial clusters and their corresponding latent variables. The collection of partial clusters is

called a partial clustering structure. The partial clustering structure describes the inherent association structure, entangled among groups of variables. Each signal z_k is represented as a linear combination of its latent variables.

Given a group of datasets $\{X_k\}_{k=1}^K$ which is a realization of $\{x_k\}_{k=1}^K$, our method exploits score subspaces from each dataset (linear subspace spanned by a set of realized vectors for each variables in the dataset) to estimate partial clusters. Specifically, the PSI quantifies the geometric relations among score subspaces via principal angles, and gathers some score subspaces within a certain angle threshold into a partial cluster. A series of estimated partial clusters then forms the estimated partial clustering structure, which is block-wise sparse. From the score subspaces in a partial cluster, we derive a partially-shared score component as a subspace average with respect to the projection Frobenius norm distance. This score component signifies a common signal direction shared in a partial cluster of interest and can be easily computed as the first right singular vector on the column-concatenation of score subspaces in the partial cluster.

Due to the heterogeneity among different data blocks, analyzing and integrating multi-source data have been a challenging subject. One of the most widely studied methods is the canonical correlation analysis (CCA) (Hotelling, 1936). CCA finds the association between two groups of variables by evaluating the maximal correlation between the linear combinations of variables in the data blocks. Our method generalizes CCA by using principal angles between score subspaces, reinterpreting the correlation measurement between linear combinations of variables in CCA.

Extensions of CCA to three or more groups of variables, called the multi-set CCA (MCCA), have been developed since Vinograd (1950); Horst (1961a,b); Meredith (1964); for comprehensive summaries, see Kettenring (1971); Nielsen (1994); Asendorf (2015).

MCCA jointly integrates all the datasets at once by solving an optimization problem on the block covariance structure. Our method steps further, not only detects the globally-shared structure which reflects the association shared by the all groups of datasets, but also identifies partially-shared structures which reflects an association shared among few of data blocks.

Another line of work is the analysis joint and individual structures (Lock et al., 2013; Feng et al., 2018; Gaynanova and Li, 2019; Gao et al., 2021; Li and Jung, 2017; Li and Gaynanova, 2018). One of the pioneering works in this area is the joint and individual variation explained (JIVE) (Lock et al., 2013). JIVE captures the joint score linear subspace and the individual score subspace specific to each data block with an iterative algorithm. The angle-based joint and individual variation explained (AJIVE) (Feng et al., 2018) improved JIVE by finding the joint structure computing the right singular vectors on the row-concatenation of every data block's right singular vector matrix with SVD. It is also an extension of the Principl Angle Analysis (PAA) (Björck and Golub, 1973) in that the computed right singular vector matrix is a subspace average among each data block's row space in the sense of the projection Frobenius-norm distance. As in AJIVE, our method exploits the concept of subspace average in finding the partial clustering structure, but generalizes JIVE and AJIVE's joint/individual segmentation by allowing partial clustering structures. While JIVE and AJIVE make use of resampling schemes in model selection, our method adopts a data splitting procedure in selecting angle threshold, which brings forth some computational advantage.

The structural learning and integrative decomposition (SLIDE) (Gaynanova and Li, 2019) and the covariate-driven blockwise sparse factorization (COBS) (Gao et al., 2021) also attempt to identify partially-shared components. Both methods find partially-shared

components via regularizing coefficients in the loading structure. In particular, SLIDE exploits the sparsity structure of each block loading using a penalized matrix factorization framework, while COBS fits a linearly structured factor model iteratively with thresholding on loading vectors, seeking for both block-wise and variable-wise sparsity. In contrast, our proposal find the block-wise structures by investigating the association in the score subspaces.

The remainder of this article is organized as follows. In Section 2, we formulate the statistical framework in view of multivariate analysis and introduce the concept of the principal entanglement structure and the principal loading matrix. In Section 3, we explain the estimation algorithms and the parameter selection procedure. In Section 4, we discuss some theoretical results. In Section 5, we present the results from numerical simulations and the comparative study with other methods. In Section 6, we implemented our method on the blood cancer multi-omics dataset associated with drug responses.

2 Statistical Framework

Consider a set of matched data matrices $X_k \in \mathbb{R}^{p_k \times n}$ for $k = 1, \dots, K$. We assume each X_k can be decomposed additively as $X_k = Z_k + E_k$ with true signal Z_k of rank r_k and error E_k . For each data source, i.e., for each k , the singular-value decomposition (SVD) of $Z_k = U_k D_k V_k^T$ gives the signal score matrix $V_k \in \mathbb{R}^{n \times r_k}$. The columns of each V_k span the r_k -dimensional subspace $[V_k]$, which we call the *score subspace* of the signal matrix Z_k .

Let $\mathcal{K} = \{1, \dots, K\}$ and consider a partially ordered set $(2^{\mathcal{K}} \setminus \{\phi\}, \subset)$ in which the order is given by the set-inclusion relation. We index all $2^K - 1$ elements of $(2^{\mathcal{K}} \setminus \{\phi\}, \subset)$, so that each $S_i \in 2^{\mathcal{K}}$ for $i \in \mathcal{I} = \{1, \dots, 2^K - 1\}$ satisfies $S_1 = \mathcal{K}$ and $j > i$ if $|S_i| > |S_j|$. The indexed partially-ordered set $(2^{\mathcal{K}} \setminus \{\phi\}, \subset)$ provides the bare structure to which we identify

the association among K data sources. Given $(2^{\mathcal{K}} \setminus \{\phi\}, \subset)$ and the score subspaces $[V_k]$, $k \in \mathcal{K}$, define the potentially joint score subspace $[W_i]$ corresponding to $S_i \in (2^{\mathcal{K}} \setminus \{\phi\}, \subset)$ in a recursive manner

$$[W_i] = \left(\bigcirc_{\substack{\{j: j < i, \\ S_j \cap S_i \neq \phi}} P_j^\perp \right) (\cap_{k \in S_i} [V_k]). \quad (1)$$

Here, P_j^\perp denotes the projection transformation of \mathbb{R}^n onto the orthogonal complement of $[W_j]$, $[W_j]^\perp$. The notation $\bigcirc_{j \in J} P_j^\perp([A])$, for an indexed set $J \subset \mathcal{I}$ and a subspace $[A]$, stands for the repeated applications of P_j^\perp on $[A]$, where P_j^\perp s are applied one by one by the increasing order of $j \in J$. Note that depending on $\{[V_k]\}$, a $[W_i]$ may be $\{0\}$.

Example 1. Suppose $K = 3$ and $\{[V_k]\}_{k \in \{1,2,3\}}$ is given. One way of ordering S_i 's is $S_1 = \{1, 2, 3\}$, $S_2 = \{1, 2\}$, $S_3 = \{2, 3\}$, $S_4 = \{1, 3\}$, $S_5 = \{1\}$, $S_6 = \{2\}$, $S_7 = \{3\}$. Upon this ordering, we construct $[W_i]$ s as $[W_1] = \cap_{k \in \{1,2,3\}} [V_k]$, $[W_2] = P_1^\perp(\cap_{k \in \{1,2\}} [V_k])$, $[W_3] = (\bigcirc_{j \in \{1,2\}} P_j^\perp)(\cap_{k \in \{2,3\}} [V_k]) = (P_2^\perp \circ P_1^\perp)(\cap_{k \in \{2,3\}} [V_k])$, $[W_4] = (\bigcirc_{j \in \{1,2,3\}} P_j^\perp)(\cap_{k \in \{1,3\}} [V_k]) = (P_3^\perp \circ P_2^\perp \circ P_1^\perp)(\cap_{k \in \{1,3\}} [V_k])$, $[W_5] = (\bigcirc_{j \in \{1,2,4\}} P_j^\perp)([V_1])$, $[W_6] = (\bigcirc_{j \in \{1,2,3\}} P_j^\perp)([V_2])$, $[W_7] = (\bigcirc_{j \in \{1,3,4\}} P_j^\perp)([V_3])$.

We call $S_i \in (2^{\mathcal{K}} \setminus \{\phi\}, \subset)$ for $i \in \mathcal{I}$ a partial cluster and $[W_i]$ the principal score subspace corresponding to S_i . The rank of a partial cluster S_i is defined as $r(S_i) = \text{rank}([W_i])$. Given $\{Z_k\}_{k \in \mathcal{K}}$ and the ordering $(2^{\mathcal{K}} \setminus \{\phi\}, \subset)$, the principal entanglement structure is the set of triples, $\mathfrak{S}(\{Z_k\}_{k \in \mathcal{K}}) = \{(S_i, r(S_i), W_i) : i \in \mathcal{I}\}$. Here, $W_i \in \mathbb{R}^{n \times r(S_i)}$ is the matrix consisting of any orthonormal basis of $[W_i]$, given that $r(S_i) > 0$. For example, the triple with $S_i = \{1, 2\}$, $r(S_i) = 2$ and $[W_i]$ means that the partially joint scores, shared only by the first and second data sources, lie in the two dimensional subspace $[W_i]$.

The principal score subspaces have the following basic property.

Lemma 1. For $i, j \in \mathcal{I}$ and $S_i \cap S_j \neq \phi$, $[W_i] \perp [W_j]$.

Note that $[W_i]$ and $[W_j]$ for $i \neq j$ are not necessarily orthogonal and the sum of principal score subspaces is exactly the sum of the score subspaces from data blocks, i.e., ${}_{i \in \mathcal{I}}[W_i] = {}_{k \in \mathcal{K}}[V_k]$, where the notation ‘+’ means the sum of subspaces.

We define the principal loading matrices that correspond to the principal score subspaces. For each $k \in \mathcal{K}$, let

$$\mathcal{I}_{(k)} = \{i : k \in S_i\} \subset \mathcal{I} \quad (2)$$

be the collection of partial cluster indices containing the k th data source. By Lemma 1, given $k \in \mathcal{K}$, the subspaces in $\{[W_i] : i \in \mathcal{I}_{(k)}\}$ are orthogonal to each other. We denote the column-wise concatenation of W_i ’s for $i \in \mathcal{I}_{(k)}$ as $W_{(k.)}$. Then $[W_{(k.)}]$ is indeed the score subspace of Z_k , that is, $[W_{(k.)}] = [V_k]$, by Lemma A.2 in the supplementary materials. Given $W_{(k.)}$, there exists a unique matrix $U_{(k)}$ such that $Z_k = U_{(k)}W_{(k.)}^T$. For each $i \in \mathcal{I}_{(k)}$, there exist $r(S_i)$ columns of $U_{(k)}$ that correspond to each W_i and this $p_k \times r(S_i)$ submatrix of $U_{(k)}$ is denoted by $U_{(k),i}$, the principal loading matrix for the k th data source associated with W_i . If $i \notin \mathcal{I}_{(k)}$, then $U_{(k),i} = 0_{p_k \times r(S_i)}$. Collecting these column vectors, the resulting overall loading matrix for the concatenated data is denoted by $U = [U_{(1)}^T, \dots, U_{(K)}^T]^T$.

Example 2. In Example 1, suppose $r(S_1) = 1$, $r(S_2) = 1$, $r(S_7) = 1$ and other partial clusters have rank zero. Then, the data sets are expressed as

$$\begin{pmatrix} X_1 \\ X_2 \\ X_3 \end{pmatrix} = \begin{pmatrix} U_{(1),1} & U_{(1),2} & 0 \\ U_{(2),1} & U_{(2),2} & 0 \\ U_{(3),7} & 0 & U_{(3),3} \end{pmatrix} \begin{pmatrix} W_1 & W_2 & W_7 \end{pmatrix}^T + \begin{pmatrix} E_1 \\ E_2 \\ E_3 \end{pmatrix} = UW^T + E.$$

It can be seen that the partial cluster $S_2 = \{1, 2\}$, for example, has the score W_2 , which is related only to the first two blocks, as shown in the second column of U .

3 Estimation Method and Algorithms

In practice, the signal Z_k and error E_k of data matrices $X_k \in \mathbb{R}^{p_k \times n}$ for $k = 1, \dots, K$ are unknown. We assume that the ranks r_k of the signal matrices are pre-determined, or pre-estimated via methods for estimating the number of factors or principal components (see e.g. Bai and Ng (2002) and references therein). We extract the signal matrix using a low-rank approximation of X_k , and write the rank r_k approximation of X_k by \widehat{Z}_k . The right singular vectors of \widehat{Z}_k spans the score subspace estimate, $[\widehat{V}_k]$.

We iterate through all partial clusters $S_i \in (\mathcal{2}^{\mathcal{K}} \setminus \{\phi\}, \subset)$ for $i = 1, \dots, 2^K - 1$, by increasing order. At the i th step, our goal is to obtain the principal score subspace estimate $[\widehat{W}_i]$ from $\{[\widehat{V}_k]\}_{k \in S_i}$. If $[\widehat{V}_k]$'s were free from noises, i.e., $[\widehat{V}_k] = [V_k]$, then we would evaluate the intersection of $[\widehat{V}_k]$'s, as in (1). However, since \widehat{Z}_k is contaminated with noises, we have $\cap_{k \in S_i} [\widehat{V}_k] = 0$ almost surely. Thus, we need to develop a method to estimate $\cap_{k \in S_i} [V_k]$, accounting for random perturbations in $[\widehat{V}_k]$.

We propose a procedure that finds a basis matrix \widehat{W}_i for the principal score subspace estimate $[\widehat{W}_i]$ at each i th step. The rank of the principal score subspace is estimated as $\widehat{r}(S_i) = \text{rank}(\widehat{W}_i)$. After estimating \widehat{W}_i and $\widehat{r}(S_i)$, we move on to the next step for S_{i+1} . Finishing the iteration over all S_i 's by the order specified in $(\mathcal{2}^{\mathcal{K}} \setminus \{\phi\}, \subset)$, we obtain the estimated principal entanglement structure $\widehat{\mathfrak{S}} = \{(S_i, \widehat{r}(S_i), \widehat{W}_i) : i \in \mathcal{I}\}$. We present the overall estimation method and algorithms in the following.

3.1 Principal Score Subspace Estimation

Fix an index $i \in \mathcal{I}$. We estimate the principal score subspace $[W_i]$ by collecting one-dimensional bases, that lie “close” to each and every score subspaces in $\{[\widehat{V}_k]\}_{j \in S_i}$. For the notion of closeness, we use a threshold parameter $\lambda \in [0, \pi/2)$ for the *principal angle*

between subspaces. For now, λ is treated as a pre-determined tuning parameter, and a data-driven choice of λ will be discussed in Section 3.3. Our algorithm for computing \widehat{W}_i consists of an iterative application of the following three steps. Briefly, the first step finds a principal direction that lies closest to all score subspaces in $\{\widehat{V}_k\}_{k \in S_i}$, using the flag mean of subspaces (Draper et al., 2014). The second step tests whether the principal direction is indeed close to each of the subspaces. If so, then the principal direction contributes to \widehat{W}_i and each \widehat{V}_k is deflated in the third step. The procedure is repeated until there is no more principal direction for S_i detected. The number of collected principal directions is $\widehat{r}(S_i)$.

We provide details of the three steps below. Throughout the process, $\{\widehat{V}_k\}$'s are deflated iteratively and can become the zero-dimensional subspace denoted by $\{0\}$. The following is applied sequentially for $i = 1, \dots, 2^K - 1$.

(a) Compute the principal direction w_i among $\{\widehat{V}_k\}_{k \in S_i}$. If any \widehat{V}_k is $\{0\}$, then skip the following and move to the next step for S_{i+1} . The principal direction minimizes the sum of the squares of the subspace distances between a candidate w and subspaces \widehat{V}_k for $k \in S_i$, and is

$$w_i = \arg \min_{w^T w = 1} \sum_{k \in S_i} d([w], [\widehat{V}_k])^2, \quad (3)$$

where $d([w], [B]) = 1/\sqrt{2} \cdot \|ww^T - BB^T\|_F$ is the Frobenius-norm distance between subspaces $[w]$ and $[B]$; see Ye and Lim (2016).

(b) Check whether the raw score subspaces are not too dispersed from w_i (3). For this, for the prespecified λ , we check the condition

$$\prod_k \mathbb{1} \left\{ \theta([w_i], [\widehat{V}_k]) < \lambda \right\} = 1. \quad (4)$$

Here, $\theta([w], [B]) = \arcsin(d([w], [B]))$ is the principal angle between subspaces $[w]$ and $[B]$; see Björck and Golub (1973); St.Thomas et al. (2014). If the condition (4)

is satisfied, then the w_i is counted as a basis for $[\widehat{W}_i]$ and we move to step (c). If not, we jump to the next step for S_{i+1} .

(c) For each $[\widehat{V}_k]$ for $k \in S_i$, we remove from $[\widehat{V}_k]$ the one-dimensional subspace that is closest to $[w_i]$ so that the result, say $[\widehat{V}_{k,trunc}]$, is orthogonal to $[w_i]$ with the dimension reduced by 1. Write $[\widehat{V}_k]$ for $[\widehat{V}_{k,trunc}]$, for each $k \in S_i$, and move back to step (a).

We give an illustrative example for the three steps.

Example 3. Assume for simplicity $n = 3$ and $S_i = \{1, 2\}$. Suppose that at this stage the deflated $[\widehat{V}_1]$ is generated by $(\cos \pi/6, 0, \sin \pi/6)^T$ and the deflated $[\widehat{V}_2]$ by $(1, 0, 0)^T$ and $(0, 1, 0)^T$; see Figure 1. Then, the step (a) computes the principal direction between $[\widehat{V}_1]$ and $[\widehat{V}_2]$, $w_i = (\cos \pi/12, 0, \sin \pi/12)^T$, as a potential estimate of a basis of $[W_i]$. Since for $k = 1, 2$, $\theta([w_i], [\widehat{V}_k]) = \pi/12$, (4) is satisfied for any tuning parameter $\lambda > \pi/12$, and we say that $[\widehat{V}_1]$ and $[\widehat{V}_2]$ share a partially joint subspace. In step (c), $[\widehat{V}_2]$ is updated to $[\widehat{V}_2] \leftarrow [\widehat{V}_{2,trunc}] = \text{span}((0, 1, 0)^T)$, and $[\widehat{V}_1]$ becomes $[\widehat{V}_1] = \{0\}$.

The principal direction vectors (3), satisfying (4), for given S_i are indexed as $\widehat{w}_i^{(j)}$ for $j = 1, \dots, \widehat{r}(S_i)$. For a singleton set $S_i = \{k\} \in (\mathcal{P}^{\mathcal{K}} \setminus \{\phi\}, \subset)$ for some $k \in \mathcal{K}$, the solution w_i is any column of \widehat{V}_k , and the condition (4) is always satisfied. Thus, for this case, $\widehat{W}_i = \widehat{V}_k$. The overall summary of the algorithm is presented in Algorithm 1.

Remark 1. In step (a), given S_i , the principal direction is obtained from the SVD of a column-wise concatenation $H \in \mathbb{R}^{n \times \sum_{k \in S_i} r_k}$ of $\{\widehat{V}_k\}_{k \in S_i}$, where r_k is the number of columns of \widehat{V}_k at the current step. By Draper et al. (2014), the objective function of (3) is

$$\sum_{k \in S_i} d \left([w], [\widehat{V}_i] \right)^2 = |S_i| - w^T \left(\sum_{k \in S_i} \widehat{V}_k \widehat{V}_k^T \right) w = |S_i| - w^T (H H^T) w,$$

and the solution w_i is the first left singular vector of H .

Algorithm 1: Iterative algorithm for partial clustering structure

input: $\widehat{V}_1, \dots, \widehat{V}_K, \lambda$

for $i = 1, 2, \dots, 2^K - 1$ **do**

 Set $\widehat{r}(S_i) = 0$ and $\mathcal{W}_i = \emptyset$;

while **do**

 Compute w_i (3) among $\{\widehat{V}_k\}_{k \in S_i} \cdot$;

if *the condition (4) is satisfied* **then**

 Let $\mathcal{W}_i \leftarrow \mathcal{W}_i \cup \{w_i\}$ and $\widehat{r}(S_i) \leftarrow \widehat{r}(S_i) + 1$;

 Update $\widehat{V}_k \leftarrow \widehat{V}_{k,trunc}$ for each $k \in S_i$;

else

 break;

end

end

 Write \widehat{W}_i for the $n \times \widehat{r}(S_i)$ matrix consisting of elements in \mathcal{W}_i and record

$(\widehat{S}_i, \widehat{r}(S_i), \widehat{W}_i)$ in $\widehat{\mathfrak{S}}$;

end

Result: $\widehat{\mathfrak{S}}$

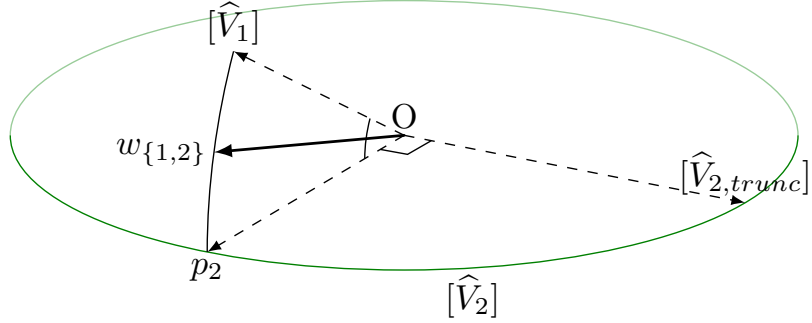


Figure 1: A figurative description for computing principal score subspace $[\widehat{W}_i]$, for $S_i = \{1, 2\}$. The two-dimensional subspace $[\widehat{V}_2]$ is depicted as a disk.

Remark 2. In step (c), for each $k \in S_i$, the one-dimensional basis of $[\widehat{V}_k]$ that is closest to $[w_i]$ is obtained as $p_k = (\widehat{V}_k \widehat{V}_k^T) w_i / \|(\widehat{V}_k \widehat{V}_k^T) w_i\|$. Let $[\widehat{V}_{k,trunc}]$ be the orthogonal complement of $[p_k]$ within $[\widehat{V}_k]$. Then, $[\widehat{V}_k]$ is updated to $[\widehat{V}_{k,trunc}]$. For a figurative illustration, see Figure 1.

3.2 Principal Loading Matrix Estimation

Given the principal entanglement structure estimate $\widehat{\mathfrak{S}}(\{\widehat{Z}_k\}_{k \in \mathcal{K}}) = \{(S_i, \widehat{r}(S_i), \widehat{W}_i) : i \in \mathcal{I}\}$, we obtain the estimated principal loading matrix \widehat{U} . Let $\widehat{Z} = (\widehat{Z}_1^T, \dots, \widehat{Z}_K^T)^T \in \mathbb{R}^{p \times n}$, where $p = \sum_{k=1}^K p_k$. We denote the column-wise concatenation of \widehat{W}_i as $\widehat{W} \in \mathbb{R}^{n \times \widehat{r}}$, where $\widehat{r} = \sum_{i=1}^{2^K-1} \widehat{r}(S_i)$. One may naively consider estimating the principal loading matrix from the optimization problem

$$\widehat{U} = \arg \min_{U \in \mathbb{R}^{p \times \widehat{r}}} \|\widehat{Z} - U \cdot \widehat{W}^T\|_F^2. \quad (5)$$

However, the estimate \widehat{U} obtained from (5) does not exhibit the block-wise sparsity structure inherited from $\widehat{\mathfrak{S}}(\{\widehat{Z}_k\}_{k \in \mathcal{K}})$; a block of \widehat{U} , say $\widehat{U}_{(k)i} \in \mathbb{R}^{p_k \times \widehat{r}(S_i)}$, for $k = 1, \dots, K$ and

$i = 1, \dots, 2^K - 1$ should be a zero matrix if $k \notin S_i$. Thus we give a constraint to (5) such that U in (5) has the block sparsity structure corresponding to the partially clustered structure in $\mathfrak{S}(\{Z_k\}_{k \in \mathcal{K}})$. For example, in the setting of Example 2, suppose that $[V_k]$'s are replaced by $[\widehat{V}_k]$'s. We constraint the optimization problem (5) so that U has a block sparsity structure

$$p_1 \left\{ \begin{bmatrix} U_{(1),1} & U_{(1),2} & 0 \\ \cdots & \cdots & \cdots \\ U_{(2),1} & U_{(2),2} & 0 \\ \cdots & \cdots & \cdots \\ U_{(3),1} & 0 & U_{(3),7} \end{bmatrix} \right. . \quad (6)$$

The objective function (5) for U can be written separately for each data block, i.e., $\|\widehat{Z} - U \cdot \widehat{W}^T\|_F^2 = \sum_{k=1}^K \|\widehat{Z}_k - U_{(k.)} \cdot \widehat{W}_{(k.)}^T\|_F^2$, where $\widehat{W}_{(k.)}$ is the column-wise concatenation of \widehat{W}_i for all $i \in \mathcal{I}_{(k)}$, and $U_{(k.)}$ is the row-concatenation of non-zero $U_{(k),i}$ blocks over $i \in \mathcal{I}_k$ (see (2) for the definition of \mathcal{I}_k). For example, in (6), $\widehat{U}_{(3.)} = [\widehat{U}_{(3),1}, \widehat{U}_{(3),7}]$, excluding the zero block. Then, each $\widehat{U}_{(k.)}$ of size $p_k \times \sum_{i \in \mathcal{I}_{(k)}} \widehat{r}(S_i)$ is computed as $\widehat{U}_{(k.)} = \widehat{Z}_k \widehat{W}_{(k.)} \left(\widehat{W}_{(k.)}^T \widehat{W}_{(k.)} \right)^{-1}$. The loading matrix estimate $\widehat{U}_{(k)} \in \mathbb{R}^{p_k \times \widehat{r}}$ for the k th data source is obtained by padding $\widehat{U}_{(k.)}$ with zero matrices for the column-blocks corresponding to $i \notin \mathcal{I}_{(k)}$ and $\widehat{r}(S_i) > 0$. The principal loading matrix estimate is $\widehat{U} = [\widehat{U}_{(1)}^T, \dots, \widehat{U}_{(K)}^T]^T$. The procedure for finding \widehat{U} is summarized in Algorithm 2.

3.3 Tuning Parameter Selection

We use data splitting to select the value of tuning parameter $\lambda \in [0, \pi/2)$. For a single instance of data splitting, split n samples of $X = [X_1^T, \dots, X_K^T]^T$ into two groups of equal proportions, the training set $X_{tr} = [X_{tr,1}^T, \dots, X_{tr,K}^T]^T$ and the test set $X_{test} = [X_{test,1}^T, \dots, X_{test,K}^T]^T$. We first determine the signal rank r_k for each dataset X_k , using `getnfac` function of R package `PANICr` with option `IC3` (Bai and Ng, 2002). We then

Algorithm 2: Finding the estimated principal loading matrix \widehat{U}

input: $\widehat{\mathfrak{S}}(\{Z_k\}_{k \in \mathcal{K}})$

for $k = 1 : K$ **do**

1. $\widehat{W}_{(k.)} \leftarrow$ the column-wise concatenation of \widehat{W}_i for all $i \in \mathcal{I}_{(k)}$;
2. $\widehat{U}_{(k.)} \leftarrow \widehat{Z}_k \widehat{W}_{(k.)} \left(\widehat{W}_{(k.)}^T \widehat{W}_{(k.)} \right)^{-1}$;
3. $\widehat{U}_k \leftarrow$ pad $\widehat{U}_{(k.)}$ with zero block matrices.

end

Result: $\widehat{U} \leftarrow [\widehat{U}_1^T | \dots | \widehat{U}_{\widehat{r}}^T]^T$

extract the training signal matrices $\widehat{Z}_{tr,k}$ for $k = 1, \dots, K$ using the rank r_k approximation of X_{tr} . Given a grid of λ 's, we perform Algorithms 1 and 2 on the training set for each λ .

Then the estimated principal loading matrix $\widehat{U}_{tr,\lambda}$ is calculated from $\widehat{Z}_{tr,k}$'s and $\widehat{W}_{tr,\lambda}$, as discussed in Section 3.2.

To assess the degrees to which the estimates are generalized to the test set, we first evaluate the score matrix for the test set, given by $\widehat{U}_{tr,\lambda}$. The test score matrix $\widehat{W}_{test,\lambda}$ is defined as the minimizer $W \in \mathbb{R}^{n_{test} \times \widehat{r}}$ of $\|X_{test} - \widehat{U}_{tr,\lambda} W^T\|_F^2$ subject to $W^T W = I_{\widehat{r}}$. The test score matrix is computed as $\widehat{W}_{test,\lambda} = P_\lambda Q_\lambda^T$, where $X_{test}^T \cdot \widehat{U}_{tr,\lambda} = P_\lambda \Sigma_\lambda Q_\lambda^T$ by the SVD, using the Eckart-Young theorem (Eckart and Young, 1936).

The best tuning parameter $\widehat{\lambda}_{best,tr}$ is the one which finds the minimum of the empirical risk, defined for $\lambda \in [0, \pi/2]$, that is,

$$\text{Risk}(\lambda) = \sum_{k=1}^K \frac{\|X_{test,k} - \widehat{U}_{tr,\lambda,(k)} \widehat{W}_{test,\lambda}^T\|_F^2}{\|X_{test,k}\|_F^2},$$

where $\widehat{U}_{tr,\lambda,(k)}$ is the k th row block of $\widehat{U}_{tr,\lambda}$. A similar form was used in Gaynanova and Li (2019). We denote the estimated principal entanglement structure for $\widehat{\lambda}_{best,tr}$ as $\widehat{\mathfrak{S}}(\{\widehat{Z}_{tr,k}\}_{k \in \mathcal{K}})$.

It turns out that simply using $\widehat{\lambda}_{best,tr}$ for the whole data does not perform well. On

the other hand, the corresponding $\widehat{\mathfrak{S}}(\{\widehat{Z}_k\}_{k \in \mathcal{K}})$ generalizes well to the whole dataset. For convenience, for any principal entanglement structure $\mathfrak{S}(\{Z_k\}_{k \in \mathcal{K}}) = \{(S_i, r(S_i), W_i) : i \in \mathcal{I}\}$, we summarize the partial clustering structure by $\mathfrak{S}_0 = \{(S_i, r(S_i)) : i \in \mathcal{I}, r(S_i) > 0\}$. For a comparison between two partial clustering structures $\widehat{\mathfrak{S}}_{0,1}$ and $\widehat{\mathfrak{S}}_{0,2}$, we use a concept of difference measure, denoted by $\text{diff}(\widehat{\mathfrak{S}}_{0,1}, \widehat{\mathfrak{S}}_{0,2})$. For this, we define the distance d_p between two partial clusters as the Hamming distance between their codified vectors. For example, $d_p(\{1, 2, 3\}, \{1, 2\}) = d_H((1, 1, 1)^T, (1, 1, 0)^T) = 1$, where d_H is the Hamming distance between two vectors. Since each partial cluster may appear multiple times, we use the multiset form $\widehat{\mathcal{S}}_0^M$ of $\widehat{\mathfrak{S}}_0$. For example, if $\widehat{\mathfrak{S}}_0 = \{(\{1, 1, 1\}, 2), (\{1, 1, 0\}, 1)\}$, then $\widehat{\mathcal{S}}_0^M = \{\{1, 1, 1\}, \{1, 1, 1\}, \{1, 1, 0\}\}$. The difference measure between a partial cluster S and a multiset $\widehat{\mathcal{S}}_0^M$ is defined as $\text{diff}(S, \widehat{\mathcal{S}}_0^M) = \min_{S' \in \widehat{\mathcal{S}}_0^M} d_p(S, S')^2$. Then the difference measure between two partial clustering structures $\widehat{\mathfrak{S}}_{0,1}$ and $\widehat{\mathfrak{S}}_{0,2}$ is defined as

$$\text{diff}(\widehat{\mathfrak{S}}_{0,1}, \widehat{\mathfrak{S}}_{0,2}) = \sum_{S \in \widehat{\mathfrak{S}}_{0,1}^M \setminus \widehat{\mathfrak{S}}_{0,2}^M} \text{diff}(S, \widehat{\mathfrak{S}}_{0,2}^M \setminus \widehat{\mathfrak{S}}_{0,1}^M) + \sum_{S \in \widehat{\mathfrak{S}}_{0,2}^M \setminus \widehat{\mathfrak{S}}_{0,1}^M} \text{diff}(S, \widehat{\mathfrak{S}}_{0,1}^M \setminus \widehat{\mathfrak{S}}_{0,2}^M). \quad (7)$$

For an illustrative example, see Section B.1 of the supplementary materials.

After estimating best parameter $\widehat{\lambda}_{best,tr}$ and its corresponding partial clustering structure, we perform Algorithm 1 on $\{\widehat{Z}_k\}$ for $k = 1, \dots, K$, the rank r_k approximations of X_k , along the grid of values of λ again. We then select the optimal parameter $\widehat{\lambda}_{whole}$ whose corresponding partial clustering structure is the closest to the best training partial clustering structure, $\widehat{\mathfrak{S}}_0(\{\widehat{Z}_{tr,k}\}_{k \in \mathcal{K}})$, in terms of the difference measure (7). The estimated principal entanglement structure for $\widehat{\lambda}_{whole}$ is denoted $\widehat{\mathfrak{S}}(\{\widehat{Z}_k\}_{k \in \mathcal{K}})$.

4 Theory

Given an ordering of partial clusters in $(2^{\mathcal{K}} \setminus \{\phi\}, \subset)$ and the signal blocks $\{Z_k : k \in \mathcal{K}\}$, the entanglement structure $\mathfrak{S}([Z_k]_{k \in \mathcal{K}}) = \{(S_i, r(S_i), W_i) : i \in \mathcal{I}\}$ is uniquely determined. Unfortunately, for different orderings of $(2^{\mathcal{K}} \setminus \{\phi\}, \subset)$, the ranks $r(S_i)$ and the principal score subspaces $[W_i]$ may be different. In this section, we introduce conditions on relations among $[V_k]$'s for $\mathfrak{S}([Z_k]_{k \in \mathcal{K}})$ to be uniquely determined regardless of the choice of the orders of $(2^{\mathcal{K}} \setminus \{\phi\}, \subset)$.

For each $l = 1, \dots, K$, let $\mathcal{J}_l = \{i \in \mathcal{I} : |S_i| = l\}$ be the set of all partial cluster indices with size l . For $l = 1, \dots, K-1$, we set $[I_l] = +_{i \in \{i:|S_i|>l\}} (\cap_{k \in S_i} [V_k]) = +_{i \in \{i:|S_i|>l\}} [W_i]$, and the projection onto $[I_l]^\perp$ in \mathbb{R}^n is denoted by $P_{I_l}^\perp$. Note that when evaluating the rank for $[W_i]$ for $i \in \mathcal{J}_l$, the definition of $[W_i]$ in (1) utilizes the deflated score subspaces orthogonal to $[I_l]$, using the given order of S_i 's among $i \in \mathcal{J}_l$. We say $\{[V_k]\}_{k \in \mathcal{K}}$ to be *relatively independent* if, for every $l = 1, \dots, K-1$ and $i \in \mathcal{J}_l$, $P_{I_l}^\perp(\cap_{k \in S_i} [V_k])$ is linearly independent to $[C_{l,-i}] = +_{j \in \mathcal{J}_l \setminus \{i\}} (P_{I_l}^\perp(\cap_{k \in S_i} [V_k]))$. In words, $\{[V_k]\}_{k \in \mathcal{K}}$ is relatively independent, if for each and every layer \mathcal{J}_l , each deflated subspace is linearly independent to $[C_{l,-i}]$, the sum of the other deflated subspaces in the layer \mathcal{J}_l . If $P_{I_l}^\perp(\cap_{k \in S_i} [V_k])$ is orthogonal to $[C_{l,-i}]$ for every $l = 1, \dots, K-1$ and $i \in \mathcal{J}_l$, then $\{[V_k]\}_{k \in \mathcal{K}}$ is said to be *relatively orthogonal*. We immediately check that relative orthogonality implies relative independence.

Theorem 1. *Given matched data matrices $X_k = Z_k + E_k \in \mathbb{R}^{p_k \times n}$ for $k = 1, \dots, K$ with true signal Z_k and error E_k , if $\{[V_k]\}_{k \in \mathcal{K}}$, the collection of Z_k 's score subspaces, is relatively independent, then, regardless of the ordering of partial clusters in $(2^{\mathcal{K}} \setminus \{\phi\}, \subset)$, there exists a unique set of pairs $\{(S_i, r(S_i))\}_{i \in \mathcal{I}}$.*

Under only the relative independence condition, the determination of the partially joint score subspaces $[W_i]$ corresponding to S_i , $i \in \mathcal{I}$, may not be unique, and depends on the

ordering of partial clusters (see Examples A.3 and A.4 in the supplementary materials). To ensure uniqueness of $[W_i]$'s, we require a rather strong assumption. We say that $\{[V_k]\}_{k \in \mathcal{K}}$ is *absolutely orthogonal*, if (1) $\{[V_k]\}_{k \in \mathcal{K}}$ satisfies relative orthogonality, and (2) for each $l = 1, \dots, K - 1$ and for every $i \in \mathcal{J}_l$,

$$P_{I_l}^\perp(\cap_{k \in S_i} [V_k]) = P_{J_i}^\perp(\cap_{k \in S_i} [V_k]), \quad (8)$$

where $[J_i] = +_{j \in \mathcal{J}_{i,>l}}(\cap_{k \in S_j} [V_k]) = +_{j \in \mathcal{J}_{i,>l}} [W_j]$ and $\mathcal{J}_{i,>l} = \{j : |S_j| > l, S_i \cap S_j \neq \emptyset\}$. In Example 1, when $l = 1$ and $i = 6$, (8) holds if $(\bigcirc_{j \in \{1,2,3,4\}} P_j^\perp)([V_1]) = (\bigcirc_{j \in \{1,2,3\}} P_j^\perp)([V_2])$. Note that for $i = 6$, $S_i = \{2\}$ and the partial clusters S_j 's for $j \in \mathcal{J}_{i,>l}$ are $S_1 = \{1, 2, 3\}$, $S_2 = \{1, 2\}$, $S_3 = \{2, 3\}$, excluding $S_4 = \{1, 3\}$.

Theorem 2. *Given matched data matrices $X_k = Z_k + E_k \in \mathbb{R}^{p_k \times n}$ for $k = 1, \dots, K$ with true signal Z_k and error E_k , if $\{[V_k]\}_{k \in \mathcal{K}}$ is absolutely orthogonal, then principal score subspaces $[W_i]$ for $i \in \mathcal{I}$ are uniquely determined.*

The uniqueness of each partially joint loading subspace $[U_{(k),i}]$ is deduced from the uniqueness of $[W_i]$'s.

Corollary 1. *Given matched data matrices $X_k = Z_k + E_k \in \mathbb{R}^{p_k \times n}$ for $k = 1, \dots, K$ with true signal Z_k and error E_k , if $\{[V_k]\}_{k \in \mathcal{K}}$ is absolutely orthogonal, then each principal loading subspace $[U_{(k),i}]$ is uniquely determined for $k = 1, \dots, K$ and $i \in \mathcal{I}_{(k)}$.*

We provide the proofs of Theorems 1 and 2 and Corollary 1 and examples for relative independence and absolute orthogonality in Section A of the supplementary materials.

5 Simulation Study

5.1 Example Dataset Generation

In the simulation study, we use the following data generation setting for numerically analyzing the performance of our proposal. Throughout, we use $K = 3$ blocks of data sets, in which the association structures are given by the ranks of partial clusters.

First, we set a pre-determined rank $r(S_i)$ for each partial cluster S_i for $i = 1, \dots, 2^K - 1$. The generic principal score matrix $W_{comp,i} \in \mathbb{R}^{n \times r(S_i)}$ for each partial cluster is a column-wise concatenation of randomly generated vectors $w_{comp,i,j}$ for $j = 1, \dots, r(S_i)$. Each $w_{comp,i,j}$ are generated element-wise and the entries of $w_{comp,i,j}$ follows $\mathcal{N}(0, \sigma_{i,j}^2)$ independently; not only independent within a $w_{comp,i,j}$, but independent between $w_{comp,i,j}$'s as well. The magnitude of signal $\sigma_{i,j}^2$'s depends on the simulation settings, and summarized as $\sigma_M^2 = \{(\sigma_{i,j}^2) : i \in \mathcal{I}, j = 1, \dots, r(S_i), r(S_i) > 0\}$. The column-wise concatenation of $W_{comp,i}$ is denoted W_{comp} of size $n \times \sum_{i=1}^{2^K-1} r(S_i)$.

The generic loading matrices $U_{comp,k,i} \in \mathbb{R}^{p_k \times r(S_i)}$ for $i = 1, \dots, 2^K - 1$ and $k = 1, \dots, K$ are made as follows. The entries of $U_{comp,k,i}$ are generated independently from the uniform distribution, $\text{Unif}(0, 1)$, and all the columns of $U_{comp,k,i}$ are scaled. We give $U_{comp,k,i}$ orthonormality by the QR decomposition. We then derive the generic signal matrix Z_k for $k = 1, \dots, K$ by $Z_k = \text{weight}_k \cdot \sum_{i=1}^{2^K-1} (U_{comp,k,i} \cdot W_{comp,i})$, where weight_k 's are weights for each dataset, which reflect the magnitude of signals. The concatenation of generic loading matrices is denoted U_{comp} , and is of size $\sum_{k=1}^K p_k \times \sum_{i=1}^{2^K-1} r(S_i)$.

The error matrix E_k is generated element-wisely, such that $e_{k,ij} \sim \mathcal{N}(0, \sigma^2)$ independently for $i = 1, \dots, p_k$ and $j = 1, \dots, n$. The magnitude of error σ^2 is given as a square root of the inverse of the signal-to-noise ratio (SNR), $\sigma^2 = 1/\text{SNR}$, where SNR is predetermined

as a simulation setting.

We use the following six models. We set $n = 200$, $p_1 = p_2 = p_3 = 100$ and $\text{weight}_1 = \text{weight}_2 = \text{weight}_3 = 1$, for all six cases. Recall that the *partial clustering structure* is given as $\mathfrak{S}_0 = \{(S_i, r(S_i)) : i \in \mathcal{I}, r(S_i) > 0\}$.

1. (Individuals) $\mathfrak{S}_0 = \{(\{1\}, 2), (\{2\}, 2), (\{3\}, 2)\}$, $\sigma_M^2 = \{(1.4, 0.8), (1.3, 0.7), (1.2, 0.6)\}$
2. (Fully joint) $\mathfrak{S}_0 = \{(\{1, 2, 3\}, 2)\}$, $\sigma_M^2 = \{(1.0, 0.9)\}$
3. (Circular, partially joint) $\mathfrak{S}_0 = \{(\{1, 2\}, 2), (\{1, 2\}, 2), (\{1, 3\}, 2)\}$, $\sigma_M^2 = \{(1.4, 0.8), (1.3, 0.7), (1.2, 0.6)\}$
4. (Mix of fully joint and individuals) $\mathfrak{S}_0 = \{(\{1, 2, 3\}, 2), (\{1\}, 2), (\{2\}, 2), (\{3\}, 2)\}$, $\sigma_M^2 = \{(1.5, 0.8), (1.4, 0.7), (1.3, 0.6), (1.2, 0.5)\}$
5. (Fully joint and partially joint) $\mathfrak{S}_0 = \{(\{1, 2, 3\}, 2), (\{1, 2\}, 2), (\{1, 3\}, 2), (\{2, 3\}, 2)\}$, $\sigma_M^2 = \{(1.5, 0.8), (1.4, 0.7), (1.3, 0.6), (1.2, 0.5)\}$
6. (All possible combinations) $\mathfrak{S}_0 = \{(\{1, 2, 3\}, 2), (\{1, 2\}, 2), (\{1, 3\}, 2), (\{2, 3\}, 2), (\{1\}, 2), (\{2\}, 2), (\{3\}, 2)\}$, $\sigma_M^2 = \{(1.8, 0.8), (1.7, 0.7), (1.6, 0.6), (1.5, 0.5), (1.4, 0.4), (1.3, 0.3), (1.2, 0.2)\}$

5.2 Results on Tuning Parameter Selection

We briefly discuss the performances of our tuning parameter selection procedure in Section 3.3 for in six models, as discussed in Section 5.1. The candidate for λ are given by $\lambda = 0^\circ, 1^\circ, \dots, 90^\circ$. For each value of λ , the empirical risk and the difference measure between the estimated and true principal entanglement structure $\widehat{\mathfrak{S}}(\{\widehat{Z}_k\}_{k \in \mathcal{K}})$ are computed.

When $\text{SNR} = 10$, `getnfrac` function estimated true signal ranks correctly for the models 1 to 5. The empirical risk is minimized at an interval of λ 's, and for any λ in the

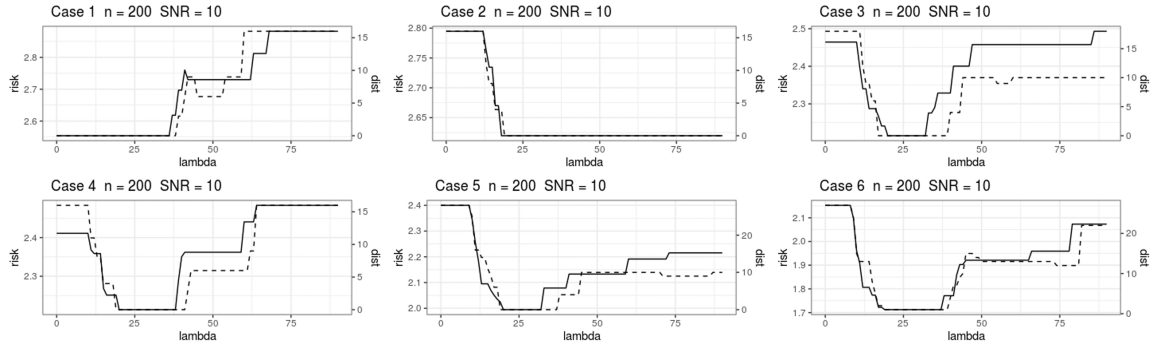


Figure 2: The values of empirical risk for λ when $n = 200$ and $\text{SNR} = 10$. Solid line : empirical risk; Dashed line : difference measure between the estimated and true structures.

interval, the corresponding partial clustering structure $\widehat{\mathfrak{S}}_0$ matches the true \mathfrak{S}_0 ; the valley bottoms of empirical risk are posited inside those of difference measure with value zero, see in Figure 2. In the model 6, the estimated true signal ranks are $r_1 = 8$, $r_2 = 8$ and $r_3 = 7$, and the estimated partial clustering structure lacks $(\{0, 0, 1\}, 1)$ from the true structure.

Meanwhile when $\text{SNR} = 2$, `getnfrac` function estimated signal ranks as zero for all six cases, so we give the true inherent signal ranks instead. Unfortunately, the empirical risk is minimized at smaller values of λ than desired; see Figure B.1 in supplementary materials. This is due to the lower value of SNR, with which the magnitude of noise overwhelms that of signal. As the score vectors of each dataset have almost random directions in low SNRs, there is a tendency that signals from a joint partial cluster score are counted separately as if they originated from different individual scores.

5.3 Results on Comparative Study

In this subsection, we numerically compare the performance of our proposal to other competitors, including SLIDE (Gaynanova and Li, 2019), COBS (Gao et al., 2021), AJIVE

(Feng et al., 2018), and JIVE (Lock et al., 2013). Note that from the estimates of each method, the principal entanglement structure \mathfrak{S} can be extracted, as well as the concatenated principal score matrix \widehat{W} and loading matrix \widehat{U} . See Section B.2 of the supplementary materials for a brief review of these methods. Our proposal will be denoted as PSI.

To assess the efficacy of finding the true partial clustering structure and proper loading and score matrices, we use the following measures.

(1) *Partial clustering structure* $\widehat{\mathfrak{S}}_0$: The rate of finding the true partial clustering, $\mathbb{E}\mathbb{1}(\mathfrak{S}_0 = \widehat{\mathfrak{S}}_0)$.

(2) *Principal loading matrix* \widehat{U} : We find the difference between U_{comp} and \widehat{U} as follows.

We denote the principal angles between $U_{comp,k,i}$ and $\widehat{U}_{(k)}$ by $\theta_{U,k,i,j}$ for $k = 1, \dots, K$, $i = 1, \dots, 2^K - 1$ and $j = 1, \dots, r(S_i)$. We report the average of all the values of $\theta_{U,k,i,j}$'s as $\bar{\theta}(U, \widehat{U})$.

(3) *Principal score matrix* \widehat{W} : We find the difference between W_{comp} and \widehat{W} as follows.

We denote the principal angle between $W_{comp,i}$ and \widehat{W} by $\theta_{W,i,j}$ for $i = 1, \dots, 2^K - 1$ and $j = 1, \dots, r(S_i)$. We report the average of all the values of $\theta_{W,i,j}$'s as $\bar{\theta}(W, \widehat{W})$.

In the comparative study, the measures $\mathbb{E}\mathbb{1}(\mathfrak{S}_0 = \widehat{\mathfrak{S}}_0)$, $\bar{\theta}(U, \widehat{U})$ and $\bar{\theta}(W, \widehat{W})$ were computed to assess the performance of PSI and other four methods. The simulation was conducted on different values of SNR (10 and 5) for the example model 1 to 6. Given a fixed true principal loading matrix U_{comp} , one hundred data sets were generated for each SNR value. We performed all 5 methods over these datasets. Average and standard deviation for each measure are reported in Tables 1 and 2.

In the example model 1, in which case there are only individual structures, PSI and AJIVE identified the true partial clustering structure for almost all instances. In the

Table 1: Comparative Study on Model 1 to 3. The unit for $\mathbb{E}1(\mathfrak{S}_0 = \widehat{\mathfrak{S}}_0)$ is percent.

Model	SNR	Measure	PSI	SLIDE bcv	COBS	AJIVE	JIVE
1	10	$\mathbb{E}1(\mathfrak{S}_0 = \widehat{\mathfrak{S}}_0)$	100 (0)	2 (14.07)	17 (37.75)	95 (21.9)	93 (25.64)
		$\bar{\theta}(U, \widehat{U})$	13.78 (0.53)	25.58 (12.48)	50.43 (10.05)	14.07 (1.86)	13.9 (0.56)
		$\bar{\theta}(W, \widehat{W})$	18.52 (0.59)	19.57 (0.72)	20.87 (1.16)	18.53 (0.55)	18.89 (0.58)
	5	$\mathbb{E}1(\mathfrak{S}_0 = \widehat{\mathfrak{S}}_0)$	99 (10)	5 (21.9)	45 (50)	96 (19.69)	83 (37.75)
		$\bar{\theta}(U, \widehat{U})$	20.22 (0.87)	37.48 (16.37)	67.2 (6.57)	20.82 (3.37)	20.42 (0.87)
		$\bar{\theta}(W, \widehat{W})$	26.21 (1.17)	28.83 (3.2)	35.07 (3.63)	26.35 (1.77)	26.38 (0.84)
2	10	$\mathbb{E}1(\mathfrak{S}_0 = \widehat{\mathfrak{S}}_0)$	100 (0)	100 (0)	100 (0)	100 (0)	62 (48.78)
		$\bar{\theta}(U, \widehat{U})$	13.01 (0.54)	13.04 (0.54)	19.39 (1.72)	60.44 (0.43)	13.05 (0.55)
		$\bar{\theta}(W, \widehat{W})$	10.95 (0.56)	11.52 (0.92)	11.26 (0.62)	10.95 (0.56)	11.5 (0.95)
	5	$\mathbb{E}1(\mathfrak{S}_0 = \widehat{\mathfrak{S}}_0)$	100 (0)	100 (0)	100 (0)	100 (0)	58 (49.6)
		$\bar{\theta}(U, \widehat{U})$	18.46 (0.8)	18.49 (0.8)	32.37 (3.02)	62.2 (0.59)	18.49 (0.81)
		$\bar{\theta}(W, \widehat{W})$	15.82 (0.85)	16.11 (1.02)	17.28 (1.14)	15.82 (0.85)	16.07 (1.04)
3	10	$\mathbb{E}1(\mathfrak{S}_0 = \widehat{\mathfrak{S}}_0)$	100 (0)	17 (37.75)	2 (14.07)	0 (0)	0 (0)
		$\bar{\theta}(U, \widehat{U})$	13.29 (0.4)	24.44 (8.74)	26.97 (5.51)	39.09 (3.61)	15.11 (2.52)
		$\bar{\theta}(W, \widehat{W})$	13.31 (0.41)	13.87 (0.52)	14.52 (0.63)	13.71 (0.78)	14.17 (0.81)
	5	$\mathbb{E}1(\mathfrak{S}_0 = \widehat{\mathfrak{S}}_0)$	100 (0)	45 (50)	9 (28.76)	0 (0)	0 (0)
		$\bar{\theta}(U, \widehat{U})$	19.20 (0.77)	33.33 (7.8)	47.61 (6.63)	47.15 (2.91)	20.89 (2.42)
		$\bar{\theta}(W, \widehat{W})$	19.17 (0.64)	19.52 (0.7)	26.13 (2.7)	20.63 (1.29)	19.89 (1.09)

example model 2, in which case there are only joint structures, all methods but JIVE find the true structure for almost all SNRs and instances. PSI and AJIVE have estimated identical score subspaces, but our method performs better in estimating loading subspaces. This is because PSI estimates the loading spaces as $\widehat{U}_k = \widehat{Z}_k \widehat{W}$, compared to AJIVE with $\widehat{U}_k = X_k \widehat{W}$, so PSI can avoid noise in computation. In the example model 3, in which partial clusters are entangled as a cyclic structure, PSI boasts superior performances in identifying the true structures.

In the example model 4, in which case both joint and individual components are composed, both PSI and AJIVE showed superior performance in identifying the true structure.

Table 2: Comparative Study on Model 4 to 6. The unit for $\mathbb{E}\mathbb{1}(\mathfrak{S}_0 = \widehat{\mathfrak{S}}_0)$ is percent.

Model	SNR	Measure	PSI	SLIDE bcv	COBS	AJIVE	JIVE
4	10	$\mathbb{E}\mathbb{1}(\mathfrak{S}_0 = \widehat{\mathfrak{S}}_0)$	100 (0)	1 (10)	19 (39.43)	100 (0)	82 (38.61)
		$\bar{\theta}(U, \widehat{U})$	13.33 (0.39)	18.6 (0.4)	35.37 (4.76)	37.59 (0.36)	13.52 (1.01)
		$\bar{\theta}(W, \widehat{W})$	17.03 (0.47)	18.03 (0.61)	19.28 (1.16)	16.99 (0.47)	17.45 (0.53)
	5	$\mathbb{E}\mathbb{1}(\mathfrak{S}_0 = \widehat{\mathfrak{S}}_0)$	100 (0)	4 (19.69)	28 (45.13)	100 (0)	53 (50.16)
		$\bar{\theta}(U, \widehat{U})$	19.65 (1.25)	29.33 (9.48)	47.92 (2.13)	41.62 (0.55)	19.51 (1.05)
		$\bar{\theta}(W, \widehat{W})$	24.37 (1.56)	28.22 (4.78)	32.84 (2.79)	24.06 (0.74)	24.32 (0.75)
5	10	$\mathbb{E}\mathbb{1}(\mathfrak{S}_0 = \widehat{\mathfrak{S}}_0)$	100 (0)	30 (46.06)	0 (0)	0 (0)	0 (0)
		$\bar{\theta}(U, \widehat{U})$	13.33 (0.38)	22.04 (6.02)	24.51 (2.22)	44.42 (2.16)	16.98 (1.39)
		$\bar{\theta}(W, \widehat{W})$	13.00 (0.34)	13.57 (0.45)	14.24 (0.52)	13.28 (0.55)	14.24 (0.53)
	5	$\mathbb{E}\mathbb{1}(\mathfrak{S}_0 = \widehat{\mathfrak{S}}_0)$	69 (46.48)	60 (49.24)	0 (0)	0 (0)	0 (0)
		$\bar{\theta}(U, \widehat{U})$	19.86 (1.85)	29.73 (5.56)	42.45 (4.34)	50.22 (1.76)	21.98 (1.45)
		$\bar{\theta}(W, \widehat{W})$	18.98 (0.85)	19.04 (0.59)	25.46 (2.18)	19.75 (0.93)	19.37 (0.77)
6	10	$\mathbb{E}\mathbb{1}(\mathfrak{S}_0 = \widehat{\mathfrak{S}}_0)$	5 (21.9)	0 (0)	0 (0)	0 (0)	0 (0)
		$\bar{\theta}(U, \widehat{U})$	16.61 (1.06)	29.92 (10.51)	32.72 (2.56)	44.1 (1.28)	18.42 (1.19)
		$\bar{\theta}(W, \widehat{W})$	20.17 (1.32)	20.27 (2.21)	24.28 (1.22)	17.47 (0.57)	18.33 (0.47)
	5	$\mathbb{E}\mathbb{1}(\mathfrak{S}_0 = \widehat{\mathfrak{S}}_0)$	0 (0)	0 (0)	0 (0)	0 (0)	0 (0)
		$\bar{\theta}(U, \widehat{U})$	27.18 (3.59)	32.42 (9.97)	46.54 (3.03)	46.13 (1.6)	24.63 (1.33)
		$\bar{\theta}(W, \widehat{W})$	30.25 (2.36)	28.25 (1.36)	33.78 (0.97)	25.62 (0.98)	25.66 (0.84)

Our method was as competent in estimating score subspaces as AJIVE. In the example model 5 and 6, the complicated cases with joint, partially joint and individual components mixed, PSI is prominent in estimating true structure, loading and score subspaces.

Our method took remarkably less computation time in almost all situations. PSI took 0.79 to 2.88 seconds in computation, compared to the time ranges from 0.87 to 22.82 seconds for SLIDE, and from 3.85 to 27.61 seconds for COBS. AJIVE took about 11 seconds consistently for all cases. JIVE exhibits the longest computation times. Table B.1 in the supplementary materials shows time comparison between our methods and other four methods.

5.4 Results on Imbalanced Signal Strength between Joint and Individual Components

Next, we consider cases where the signal strengths of joint structures and individual structures are grossly imbalanced. Consider a new model, with $K = 3$ and $p_1 = p_2 = p_3 = 100$, whose partial cluster ordering is $S_1 = \{1, 2, 3\}$, $S_5 = \{1\}$, $S_6 = \{2\}$ and $S_7 = \{3\}$. We set inherent joint rank $r(S_1) = 10$ and individual ranks $r(S_5) = r(S_6) = r(S_7) = 10$. Other partial clusters have zero ranks, $r(S_2) = r(S_3) = r(S_4) = 0$. Through out, $n = 200$.

For the case in which there are larger variations in the joint component than the individual components, we set $\sigma_{1,j}^2 \gg \sigma_{i,j}^2$ for $i = 5, 6, 7$ and all j 's. In the opposite case, we give larger variations in the individual components than the joint component, $\sigma_{i,j}^2 \gg \sigma_{1,j}^2$ for $i = 5, 6, 7$ and all j 's. Details are given in Section B.4 of the supplementary materials.

We carried out comparative simulations on both cases at SNR levels ∞ and 5. Not only the success rate of finding true structure but also the numbers of estimated joint and individual structures were evaluated. In Table 3, in which case the joint component has larger variations, JIVE showed superior performances to other methods, but PSI is also compatible in identifying joint and individual components. PSI did not succeed in identifying individual components for SNR = 5, because initial rank estimations failed to distinguish the weak individual signals from noise. When the individual components have larger variations, in Table 4, our method shows more robust performances in finding both joint and individual components than other methods.

Table 3: The case where the joint component has larger variations than the individual components.

SNR	Measure	PSI	SLIDE bcv	COBS	AJIVE	JIVE
∞	$\mathbb{E}1(\mathfrak{S}_0 = \widehat{\mathfrak{S}}_0)$	31 (46)	0 (0)	0 (0)	0 (0)	92 (27.27)
	Joint	10 (0)	10 (0)	39.46 (0.82)	4 (2.01)	9.92 (0.27)
	Individual	32.3 (2.56)	0 (0)	0.04 (0.24)	48 (6.02)	27.84 (7.36)
5	$\mathbb{E}1(\mathfrak{S}_0 = \widehat{\mathfrak{S}}_0)$	0 (0)	0 (0)	0 (0)	0 (0)	4 (19.69)
	Joint	10 (0)	10 (0)	13.08 (1.67)	10 (0)	9.92 (0.27)
	Individual	0 (0)	0 (0)	17.98 (2.6)	32.53 (0.9)	32.05 (10.27)

Table 4: The case where the individual components have larger variations than the joint components.

SNR	Measure	PSI-MDI	SLIDE bcv	COBS	AJIVE	JIVE
∞	$\mathbb{E}1(\mathfrak{S}_0 = \widehat{\mathfrak{S}}_0)$	78 (41.63)	0 (0)	0 (0)	0 (0)	0 (0)
	Joint	10 (0)	0.23 (0.47)	38.86 (1.11)	3.94 (1.73)	3.46 (1.38)
	Individual	30.4 (0.89)	26.86 (1.14)	0.05 (0.26)	48.18 (5.2)	27.82 (1.31)
5	$\mathbb{E}1(\mathfrak{S}_0 = \widehat{\mathfrak{S}}_0)$	0 (0)	0 (0)	0 (0)	0 (0)	0 (0)
	Joint	6.05 (1.73)	0.68 (0.68)	31.26 (2.75)	0.92 (0.54)	2.88 (1.21)
	Individual	35.09 (3.45)	28.93 (1.77)	2.73 (1.51)	57.26 (1.64)	27.91 (1.32)

6 Real Data Analysis

In recent days, individualized therapeutics became vital in effective cancer treatment. In many cancers, patients show heterogeneous responses to anti-cancer drugs, that is, there are suspected hidden clusters of patients that show different response patterns to the drugs, which hamper the precise prediction of each patient's drug responses. We wish to discover quintessential biomarkers which can explain the heterogeneity of drug response patterns and provide a more precise and systematic therapeutic strategy. Multi-omics genetic profiles of

the primary cancer cell associated with a drug response panel lead to a powerful insight in finding useful biomarkers.

In this section, we apply our PSI method to the dataset EGAS0000100174, a blood cancer multi-omics data linked to a drug response panel (Dietrich et al., 2018). We have chosen to use 121 cases diagnosed with chronic lymphocytic leukemia (CLL). The drug response panel (X_{Drug}) records the *ex vivo* cell viabilities at a series of 5 concentrations, for each of 62 drugs which target onco-related pathways or are used widely in clinical practice. The multi-omics dataset consists of the genome-wide DNA methylation profiles and the RNA sequencing profiles. The top 5,000 most variable CpG sites were selected (X_{Meth}) from the *450K illumina assay* DNA methylation profile. As for the RNA sequencing profile, we selected the top 5,000 gene expressions with the largest stabilized variances (X_{Exp}) from the high-throughput sequencing (HTS) assay. In summary, we have multiple datasets $X_{\text{Drug}} \in \mathbb{R}^{121 \times 310}$, $X_{\text{Meth}} \in \mathbb{R}^{121 \times 5000}$ and $X_{\text{Exp}} \in \mathbb{R}^{121 \times 5000}$. We presumbaly truncated each dataset by the SVD at an inherent rank that explain 60.8%, 60.4%, 68.4% of variation for Drug, Meth and Exp datasets, that is, $r_1 = 5$, $r_2 = 42$ and $r_3 = 3$; see Figure C.1 in supplementary materials.

We repeat the estimation process over 100 repetitions and select the mode structure, that is, the estimated partial clustering structure that appears the most out of 100 repetitions. The estimated mode structure is

$$\widehat{\mathfrak{S}}_0 = \{(\{1, 1, 0\}, 1), (\{1, 0, 0\}, 4), (\{0, 1, 0\}, 41), (\{0, 0, 1\}, 3)\},$$

which means that the PSI detected the partial cluster $\{1, 1, 0\}$ of rank 1, and no fully joint cluster $\{1, 1, 1\}$ or other forms of partial clusters were detected. This structure appeared 53 times out of 100 repetitions. In an Intel ® Xeon ® CPU E5-2640 v4 @ 2.40GHz system, it took 9.38 seconds per single data splitting instance (54.56 seconds for 100 instances

with 40 cores). In comparison, the SLIDE with bcr method detected the same structure as our method, but it took almost 9 hours on the same machine. The COBS yielded an eccentric result, $\{1, 1, 1\}$ of rank 50, taking about 14 minutes. The detection of the partial cluster $\{1, 1, 0\}$ was also robust over different choices of initial ranks. When each dataset is truncated by the SVD at levels 30%, 40% and 50% (inherent signal ranks are $(2, 6, 1)$, $(2, 15, 1)$ and $(3, 28, 2)$ for each), the PSI detected the same partial cluster $\{1, 1, 0\}$ of rank 1.

The reconstructed matrices for the partial clusters are plotted in Figure 3. Both the samples and the variables of X_{Drug} are ordered by a hierarchical bi-clustering applied to the component of X_{Drug} corresponding to the partial cluster $\{1, 1, 0\}$, denoted X_{Drug}^{110} , shown in the top left part of Figure 3. The variables of X_{Meth} are similarly ordered. Focusing on the partial cluster $\{1, 1, 0\}$, the samples are clustered into two distinct subgroups, denoted by Groups α and β , see Figure 4(a). The variables in X_{Drug} and X_{Meth} show a contrasting pattern according to the subgroups α and β .

Comparing X_{Drug}^{110} (see Figure 4(a)) with the whole X_{Drug} (see Figure 4(b)), we observe that the clusters identified above are hidden in X_{Drug} . Moreover, the subgroups α and β are well-separated in the score subspace of X_{Drug}^{110} (see Figure 4(c)), while it is hard to discern two subgroups in the whole X_{Drug} (see Figure 4(d)). The same conclusion can be made by inspecting the component of X_{Meth} corresponding to the partial cluster $\{1, 1, 0\}$, denoted X_{Meth}^{110} , and the whole X_{meth} in Figure 4(e) and (f). Thus we here observed that the PSI gives a more effective measure in finding an inherent sample subgroup structure of given multi-omics datasets than a naive application of the PCA on each data matrix.

To find indicators that best explain the subgroups α and β , we conducted the Fisher exact test simultaneously on 59 gene mutations or chromosome defects of each patients,

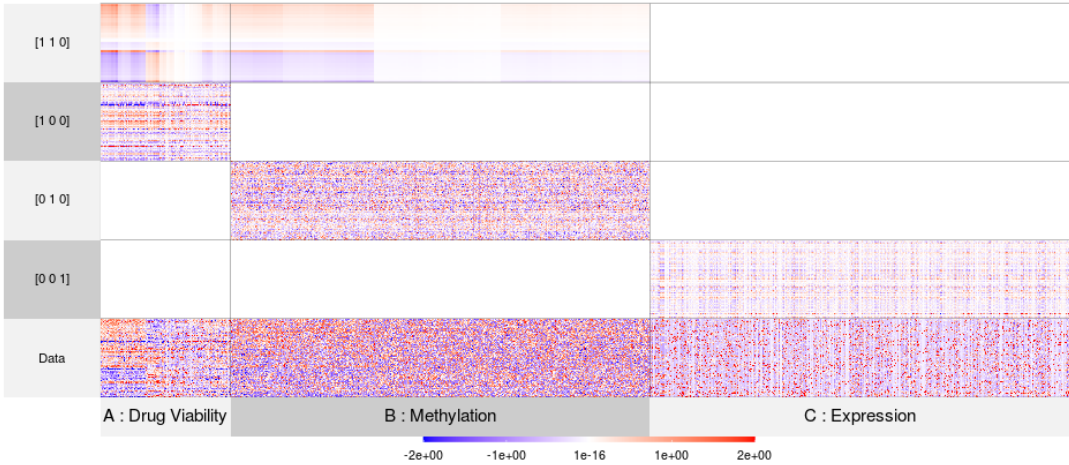


Figure 3: The reconstructed matrices for partial clusters; The values are all normalized for each column, then truncated to line on $[-2, 2]$.

available as an ancillary information. The p-values from each Fisher exact test were adjusted by the Benjamini-Hochberg (BH) method. The smaller p-values indicate stronger differences of each mutation or chromosome defect between the subgroup α and β . We found that the immunoglobulin heavy chain variable (IGHV) region mutation status has the most associated relation with the subgroups at BH-adjusted p-value 1.026×10^{-13} . We also present the 2×2 table of the IGHV status and the subgroups, see Tables C.1 and C.2 in the supplementary materials. We postulate IGHV mutation status gives a substantial explanation for the subgrouping of CLL patients, that is, wild type matches to the subgroup α and mutation type to the subgroup β . Survival analyses on overall survival was also conducted, and there are statistically significant differences in survival between the two subgroups α and β as shown in Figure 5.

Again in Figure 4(a), the variables of X_{Drug}^{110} can be clustered into subgroups [a] and [b] showing a contrasting response pattern to the subgroups α and β (variables showing weak responses were excluded as subgroup [c]). The subgroup [a] shows higher viability for β

(IGHV mutated) than α (IGHV wild type) and vice versa for [b]. Table C.3 (in supplementary materials) presents the list of prominent drugs that have appeared in subgroups [a] and [b] at least 4 times out of 5 concentrations. For the subgroup [a], the table lists a number of inhibitor drugs that target the B cell receptor (BCR) components, such as Bruton's tyrosine kinase (BTK; spebrutinib, ibrutinib), phosphatidylinositol 3-kinase (PI3K; idelalisib, duvelisib) and spleen tyrosine kinase (STK; tamatinib, PRT062607 HCL). AKT inhibitor (MK-2206) or SRC inhibitors (dasatinib) targets signal transduction pathways that promotes survival and growth of B cell lymphocytes. Unexpected encounter with HSP90 inhibitor (AT13387 or Onalespib) may be related to the stability of lymphocyte-specific SRC family kinases (Mshaik et al., 2021). The appearance of CHK inhibitors (PF 477736, AZD7762, CCT241533) may be linked to repairing mechanisms of DNA damages at G2 phase, known to be associated with WEE1 kinase and the AKT/PKB pathway (Zhang and Hunter, 2014). For the subgroup [b], the appearance of mTOR inhibitor (everolimus) may suggest that mTOR pathway and shows different drug sensitivities to the BCR component, despite the fact that it is on the downstream of AKR/PKB pathway. The role of IGHV in this implication requires further investigation. BCL2 inhibitor (navitoclax) and rotenone might be related to the role of mitochondria in apoptosis (Wang and Youle, 2014).

Supplementary Materials

The supplementary materials contain the proofs of Theorem 1 and 2, the settings of simulation study, a brief review on competing methods, additional simulation results, additional information on real data analysis, and a table of drugs selected by the PSI.

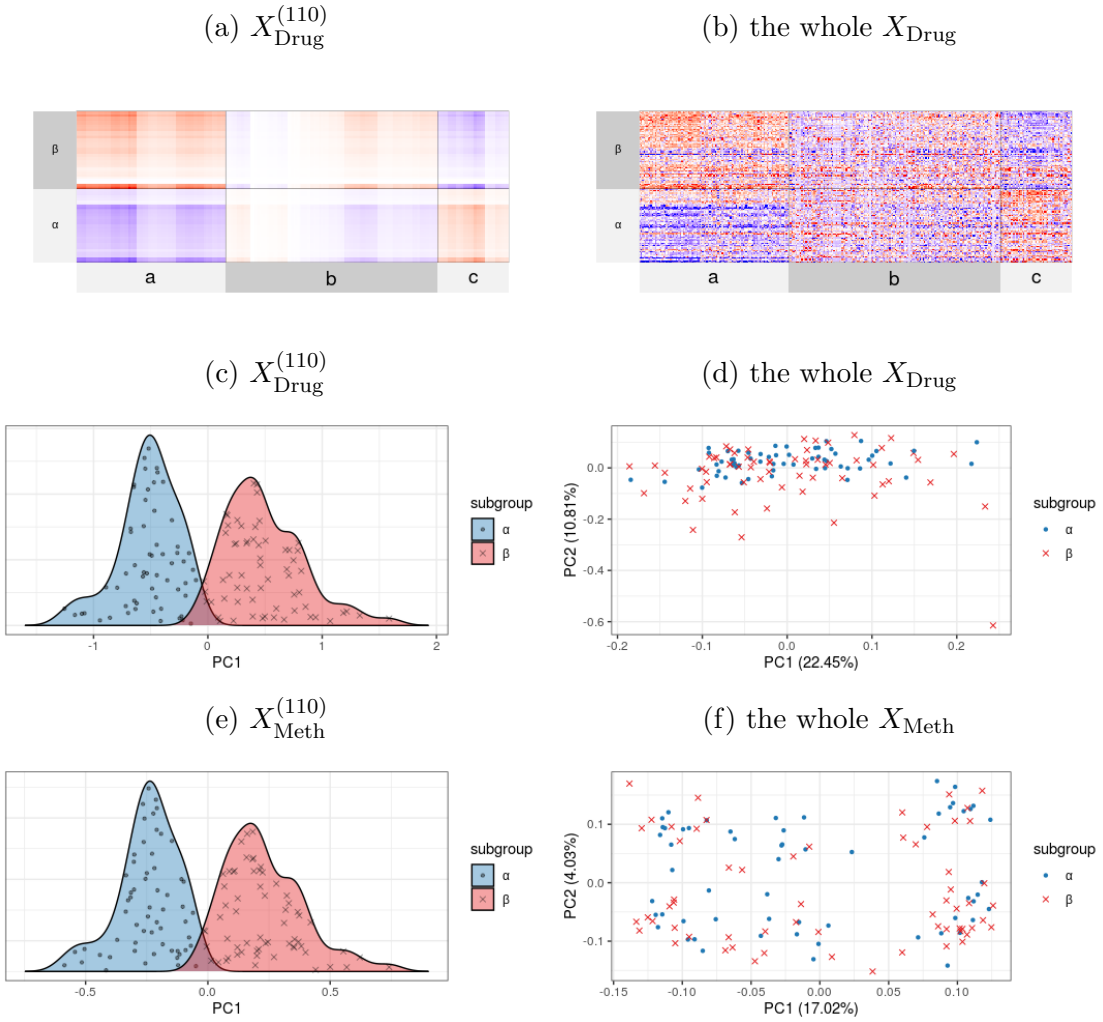


Figure 4: (a) In the component of X_{Drug} corresponding to the partial cluster $\{1, 1, 0\}$, denoted $X_{\text{Drug}}^{(110)}$; (b) The whole X_{Drug} data matrix; (c) The density plot of the subgroups α and β along the first principal component of $X_{\text{Drug}}^{(110)}$; (d) The PC plots of the whole X_{Drug} ; (e) The density plot of the subgroups α and β along the first principal component of $X_{\text{Meth}}^{(110)}$; (f) The PC plots of the whole X_{Meth} .

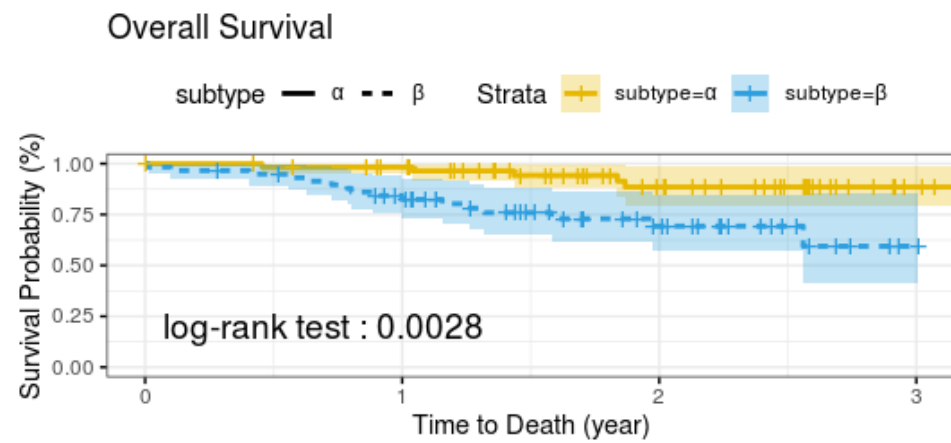


Figure 5: The difference in overall survival between the subgroups α and β is displayed on a Kaplan plot with p-value 0.0028 from the log-rank test.

References

Asendorf, N. A. (2015). *Informative data fusion: Beyond canonical correlation analysis*. Ph. D. thesis, University of Michigan.

Bai, J. and S. Ng (2002). Determining the number of factors in approximate factor models. *Econometrika* 70(1), 191–221.

Björck, A. and G. Golub (1973). Numerical methods for computing angles between linear subspaces. *Mathematics of Computation* 27(123), 579–594.

Dietrich, S., M. Oleś, J. Lu, L. Sellner, and et al. (2018). Drug-perturbation-based stratification of blood cancer. *Journal of Clinical Investigation* 128(1), 427–445.

Draper, B., M. Kirvy, J. Marks, T. Marrinan, and C. Peterson (2014). A flag representation for finite collections of subspaces of mixed dimensions. *Linear Algebra and its Applications* 451, 15–32.

Eckart, C. and G. Young (1936). The approximation of one matrix by another of lower rank. *Psychometrika* 1, 211–218.

Feng, Q., M. Jiang, J. Hannig, and J. Marron (2018). Angle-based joint and individual variation explained. *Journal of Multivariate Analysis*, 241–265.

Gao, X., S. Lee, and S. Jung (2021). Covariate-driven factorization by thresholding for multi-block data. *Biometrics* 77(3), 1011–1023.

Gaynanova, I. and G. Li (2019). Structural learning and integrative decomposition of multi-view data. *Biometrics* 75, 1121–1132.

Horst, P. (1961a). Generalized canonical correlations and their applications to experimental

data. *Journal of Clinical Psychology* 72(2), 331 – 347.

Horst, P. (1961b). Relations among sets of measures. *Psychometrika* 26(2), 129 – 149.

Hotelling, H. (1936). Relations between two sets of variates. *Biometrika* 28(3/4), 321–377.

Kettenring, J. R. (1971). Canonical analysis of several sets of variables. *Biometrika* 58, 433–451.

Li, G. and I. Gaynanova (2018). A general framework for association analysis of heterogeneous data. *The Annals of Applied Statistics* 12(3), 1700–1726.

Li, G. and S. Jung (2017). Incorporating covariates into integrated factor analysis of multi-view data. *Biometrics* 72, 1433–1442.

Lock, E., K. Hoadley, J. Marron, and A. Nobel (2013). Joint and individual variation explained (jive) for integrated analysis of multiple data types. *Annals of Application Statistics* 7(1), 523–542.

Meredith, W. (1964). Rotation to achieve factorial invariance. *Psychometrika* 29(2), 187 – 206.

Mshaik, R., J. Simonet, A. Georgievski, and et al. (2021). Hsp90 inhibitor nvp-bep800 affects stability of src kinases and growth of t-cell and b-cell acute lymphoblastic leukemias. *Blood Cancer Journal* 11(61).

Nielsen, A. A. (1994). *Analysis of Regularly and Irregularly Sampled Spatial, Multivariate, and Multi-temporal Data*. Ph. D. thesis, Institute of Mathematical Modelling / Technical University of Denmark, Lyngby, Denmark.

Norris, J. L., M. A. Farrow, D. B. Gutierrez, et al. (2017). Integrated, high-throughput, multiomics platform enables data-driven construction of cellular responses and reveals global drug mechanisms of action. *Journal of Proteome Research* 16(3), 1364–1375.

Reuter, J. A., D. Spacek, and M. P. Snyder (2015). High-throughput sequencing technologies. *Molecular Cell* 58(4), 586–597.

St.Thomas, B., L. Lin, L.-H. Lim, and S. Mukherjee (2014). Learning subspaces of different dimensions. arXiv:1404.6841.

Subramanian, I., S. Verma, S. Kumar, A. Jere, and K. Anamika (2020). Multi-omics data integration, interpretation, and its application. *Bioinformatics and Biology Insights*.

Vershynin, R. (2018). *High-dimensional Probability* (1 ed.). Cambridge University Press.

Vinograde, B. (1950). Canonical positive definite matrices under internal linear transformations. *Proceedings of American Mathematical Society* 1, 159–161.

Wang, C. and R. J. Youle (2014). The role of mitochondria in apoptosis. *Annu Rev Genet.* 43, 95–118.

Ye, K. and L.-H. Lim (2016). Schubert varieties and distances between subspaces of different dimensions. *SIAM Journal of Matrix Analysis and Applications* 37(3), 1176–1197.

Zhang, Y. and T. Hunter (2014). Roles of chk1 in cell biology and cancer therapy. *International Journal of Cancer* 134(5), 1013–1023.

Principal Structure Identification: Fast Disentanglement of Multi-source Dataset

SUPPLEMENTARY MATERIAL

A Proofs

A.1 Proof of Lemma 1

Proof. From the definition of the principal direction, we immediately find that

$$[W_i] \perp [W_j], \quad i, j \in \mathcal{I} \text{ and } S_j \cap S_i \neq \emptyset$$

by the range-kernel complementarity property of the vector space projection transformation. \square

A.2 Proof of Theorem 1

Proof. We claim that $\text{rank}([W_i])$ is uniquely determined. By Sylvester's law of nullity, we have

$$\text{rank}([W_i]) = \text{rank}(\bigcap_{k \in S_i} [V_k]) - \text{rank}(\mathcal{N}(\bigcirc_{j \in \mathcal{I}_{< i}} P_j^\perp) \cap (\bigcap_{k \in S_i} [V_k])),$$

where $\mathcal{I}_{< i} = \{j : j < i, S_j \cap S_i \neq \emptyset\}$. Hereafter $\mathcal{N}(T)$ is the null space of a transformation T of \mathbb{R}^n and $\mathcal{R}(T)$ its range space. We first suggest the following lemmata.

Lemma 2. *For $i \in \mathcal{I}$, we have $\mathcal{N}(\bigcirc_{k \in \mathcal{I}_{< i}} P_k^\perp) = \bigoplus_{k \in \mathcal{I}_{< i}} [W_k]$.*

Proof. Let $v \in \bigoplus_{k \in \mathcal{I}_{< i}} [W_k]$. Then there exists a unique $\{v_k\}_{k \in \mathcal{I}_{< i}}$ with $v_k \in [W_k]$ such that the sum of all v_k is v . For each $j_1 \in \mathcal{I}_{< i}$ and $v_{j_1} \in [W_{j_1}]$, it can be easily checked that

$(\bigcirc_{k \in \mathcal{I}_{<j_1}} P_k^\perp)(v_{j_1}) = \{0\}$ and then $(\bigcirc_{k \in \mathcal{I}_{<i}} P_k^\perp)(v_{j_1}) = \{0\}$ follows. Thus $(\bigcirc_{k \in \mathcal{I}_{<i}} P_k^\perp)(v) = \{0\}$ and $\mathcal{N}(\bigcirc_{k \in \mathcal{I}_{<i}} P_k^\perp) \supset \bigoplus_{k \in \mathcal{I}_{<i}} [W_k]$.

Conversely, let $v' \notin \bigoplus_{k \in \mathcal{I}_{<i}} [W_k]$. Then there exists a unique $\{v_k\}_{k \in \mathcal{I}_{<i}}$ with $v_k \in [W_k]$ and non-zero $a \in (\bigoplus_{k \in \mathcal{I}_{<i}} [W_k])^\perp$ such that v' is the sum of all v_k and a . For each $j_1 \in \mathcal{I}_{<i}$ and $v_{j_1} \in [W_{j_1}]$, we have $(\bigcirc_{k \in \mathcal{I}_{<i}} P_k^\perp)(v_{j_1}) = \{0\}$ as before. Since $a \perp [W_{k''}]$ for any $k'' \in \mathcal{I}_{<i}$, we also have $(\bigcirc_{k \in \mathcal{I}_{<i}} P_k^\perp)(a) \neq 0$. Thus we have $(\bigcirc_{k \in \mathcal{I}_{<i}} P_k^\perp)(v') \neq \{0\}$ and $\mathcal{N}(\bigcirc_{k \in \mathcal{I}_{<i}} P_k^\perp) \subset \bigoplus_{k \in \mathcal{I}_{<i}} [W_k]$. \square

Lemma 3. For $i \in \mathcal{I}$, we have $\bigoplus_{k \in \mathcal{I}_{<i}} [W_k] = \bigoplus_{k \in \mathcal{I}_{<i}} (\bigcap_{k' \in S_k} [V_{k'}])$.

Proof. We give a proof by induction on k . If $k = 1$, there is nothing to prove. If $k = 2$, $[W_1] = \bigcap_{k' \in S_1} [V_{k'}]$, so the statement is true for $k = 1, 2$.

For any $k \geq 3$, suppose the statement holds, that is,

$$\bigoplus_{j \in \mathcal{I}_{<m}} [W_j] = \bigoplus_{j \in \mathcal{I}_{<m}} (\bigcap_{k' \in S_j} [V_{k'}])$$

for all $1 \leq m \leq k$. Let \tilde{k} be the largest element in $\mathcal{I}_{<k+1}$. We denote $P = \bigcirc_{k' \in \mathcal{I}_{<\tilde{k}}} P_{k'}^\perp$ and P^\perp , the projection onto $\mathcal{N}(P)$ of \mathbb{R}^n . Then, we have

$$\begin{aligned} \bigoplus_{j \in \mathcal{I}_{<k+1}} (\bigcap_{k' \in S_j} [V_{k'}]) &= \bigoplus_{j \in \mathcal{I}_{<\tilde{k}}} [W_j] + \bigcap_{k' \in S_{\tilde{k}}} [V_{k'}] \\ &= \bigoplus_{j \in \mathcal{I}_{<\tilde{k}}} [W_j] + P(\bigcap_{k' \in S_{\tilde{k}}} [V_{k'}]) + P^\perp(\bigcap_{k' \in S_{\tilde{k}}} [V_{k'}]) \end{aligned}$$

Indeed, $P^\perp(\bigcap_{k' \in S_{\tilde{k}}} [V_{k'}]) \subset \mathcal{N}(P)$ and $\mathcal{N}(P) = \bigoplus_{k' \in \mathcal{I}_{<\tilde{k}}} [W_{k'}]$ by the previous lemma. Thus

$$\begin{aligned} \bigoplus_{j \in \mathcal{I}_{<k+1}} (\bigcap_{k' \in S_j} [V_{k'}]) &= \bigoplus_{j \in \mathcal{I}_{<\tilde{k}}} [W_j] + P(\bigcap_{k' \in S_{\tilde{k}}} [V_{k'}]) \\ &= \bigoplus_{j \in \mathcal{I}_{<\tilde{k}}} [W_j] \oplus [W_{\tilde{k}}] \\ &= \bigoplus_{j \in \mathcal{I}_{<k+1}} [W_j]. \end{aligned}$$

Therefore the statement holds for any $k \geq 3$ and the proof is completed. \square

Circling back to the main story, Sylvester's law of nullity for our theorem is restated as

$$\text{rank}([W_i]) = \text{rank}(\cap_{k \in S_i} [V_k]) - \text{rank}((+_{k \in \mathcal{I}_{< i}} (\cap_{k' \in S_k} [V_{k'}])) \cap (\cap_{k \in S_i} [V_k])).$$

We want to make this expression in a more explicit form. For that, we suggest the following assertions.

Let $l = |S_i|$. We set $[I_l] = +_{k \in \{k : |S_k| > l\}} (\cap_{k' \in S_k} [V_{k'}])$. The projection onto $[I_l]$ in \mathbb{R}^n is denoted by P_{I_l} and the projection onto $[I_l]^\perp$ is denoted by $P_{I_l}^\perp$. Moreover, we consider an index set $\mathcal{J}_{i,>l} = \mathcal{I}_{< i} \cap \{k : |S_k| > l\}$ and let $[J_i] = +_{k \in \mathcal{J}_{i,>l}} (\cap_{k' \in S_k} [V_{k'}])$. The projection onto $[J_i]$ in \mathbb{R}^n is denoted by P_{J_i} and the projection onto $[J_i]^\perp$ by $P_{J_i}^\perp$. Finally, we define $\mathcal{J}_{i,l} = \mathcal{I}_{< i} \cap \{k : |S_k| = l\}$.

Lemma 4. $P_{I_l}^\perp = P_{I_l}^\perp \circ P_{J_i}^\perp$.

Proof. Trivial from the fact $\mathcal{N}(P_{J_i}^\perp) \subset \mathcal{N}(P_{I_l}^\perp)$. \square

Lemma 5. *If $v_j \in P_{J_i}^\perp (\cap_{k' \in S_j} [V_{k'}])$ with $j \in \mathcal{J}_{i,l} \setminus \mathcal{J}'_{i,l}$, then $v_j \in (\cap_{k' \in S_j} [V_{k'}]) \cap (\cap_{k' \in S_m} [V_{k'}])$ for some $m < i$, $m \neq j$ such that $S_m \cap S_i = \{0\}$ and not for any $m < i$, $m \neq j$ such that $S_m \cap S_i \neq \{0\}$.*

Proof. Consider the cases

(1) $v_j \in (\cap_{k' \in S_j} [V_{k'}]) \cap (\cap_{k' \in S_m} [V_{k'}])$ for some $m < i$, $m \neq j$ such that $S_m \cap S_i \neq \{0\}$ but not for any $S_m \cap S_i = \{0\}$,

(2) $(\cap_{k' \in S_j} [V_{k'}]) \cap (\cap_{k' \in S_m} [V_{k'}]) = \{0\}$ for only $m \in \mathcal{J}_{i,l}$

In case (1), v_j becomes automatically an element of $\cap_{k' \in S_t} [V_{k'}]$ such that $S_j \subset S_t$ and $S_m \subset S_t$. Then $v_j \in [I_i]$ since $S_i \cap S_t \neq \emptyset$ and $|S_t| > |S_i|$, and this is a contradiction. In case (2), $v_j \notin \mathcal{R}(P_{I_l})$ and this is contradict to the assumption. \square

Proposition 1. *If $[V_k]_{k \in \mathcal{K}}$ is relatively independent, then ${}_{+k \in \mathcal{J}_{i,l}} P_{J_i}^\perp(\cap_{k' \in S_k} [V_{k'}])$ and $P_{J_i}^\perp(\cap_{k \in S_i} [V_k])$ are independent.*

Proof. We want to show that the relative independence of $[V_k]_{k \in \mathcal{K}}$ is violated if ${}_{+k \in \mathcal{J}_{i,l}} P_{J_i}^\perp(\cap_{k' \in S_k} [V_{k'}])$ and $P_{J_i}^\perp(\cap_{k \in S_i} [V_k])$ are linearly dependent. Suppose that there is nonzero $v \in {}_{+k \in \mathcal{J}_{i,l}} P_{J_i}^\perp(\cap_{k' \in S_k} [V_{k'}]) \cap P_{J_i}^\perp(\cap_{k \in S_i} [V_k])$ with $l = |S_i|$. We are going to show that ${}_{+k \in \mathcal{J}_{i,l}} P_{J_i}^\perp(\cap_{k' \in S_k} [V_{k'}]) \cap P_{J_i}^\perp(\cap_{k \in S_i} [V_k])$ is not $\{0\}$ in the following cases.

First we exclude the case where $P_{I_l}^\perp(\cap_{k' \in S_i} [V_{k'}]) = \{0\}$. If so we have $\cap_{k' \in S_i} [V_{k'}] = \bigoplus_{k'' \in \{k'': S_i \subset S_{k''}\}} [W''_{k''}] = {}_{+k'' \in \{k'': S_i \subset S_{k''}\}} [V''_{k''}]$, then $\cap_{k' \in S_i} [V_{k'}]$ itself is in $[I_i] = \mathcal{N}(P_{J_i}^\perp)$.

Next, under the assumption that $P_{I_l}^\perp(\cap_{k' \in S_i} [V_{k'}]) \neq \{0\}$, we run through the following situations. Now on $\mathcal{J}'_{i,l} = \{k : |S_k| = l, k \in \mathcal{I}_{< i}, P_{I_i}^\perp(S_k) \neq \{0\}\}$.

(i) $|\mathcal{J}_{i,l}| = 0$: There is nothing to prove.

(ii) $|\mathcal{J}_{i,l}| = 1$ and $|\mathcal{J}'_{i,l}| = 0$:

We will show that this case is vacuous. Suppose there exist nonzero $v \in P_{J_i}^\perp(\cap_{k' \in S_i} [V_{k'}]) \cap P_{J_i}^\perp(\cap_{k' \in S_k} [V_{k'}])$ with $k \in \mathcal{J}_{i,l}$. As $P_{I_l}^\perp(\cap_{k' \in S_k} [V_{k'}]) = \{0\}$, we can deduce that $P_{I_l}^\perp(v) = 0$.

We pick a vector u in $\cap_{k' \in S_j} [V_{k'}]$ such that $S_i \subset S_j$ and $S_j \subset S_i$. As $\cap_{k' \in S_j} [V_{k'}] \subset \cap_{k' \in S_i} [V_{k'}]$ and $\cap_{k' \in S_j} [V_{k'}] \subset \cap_{k' \in S_k} [V_{k'}]$, we have $u \in (\cap_{k' \in S_i} [V_{k'}]) \cap (\cap_{k' \in S_k} [V_{k'}])$. As $S_i \cap S_j \neq \emptyset$, we observe that $\cap_{k' \in S_j} [V_{k'}] \subset [I_i] = \mathcal{N}(P_{J_i}^\perp)$.

$$\begin{aligned} u &\in P_{J_i}((\cap_{k' \in S_i} [V_{k'}]) \cap (\cap_{k' \in S_k} [V_{k'}])) \\ &\subset P_{J_i}(\cap_{k' \in S_i} [V_{k'}]) \cap P_{J_i}(\cap_{k' \in S_k} [V_{k'}]). \end{aligned}$$

Let $w = u + v$. Since $u \in P_{J_i}(\cap_{k' \in S_k} [V_{k'}])$ and $v \in P_{J_i}^\perp(\cap_{k' \in S_k} [V_{k'}])$ with respect to S_k and the same for S_i , we find that $w \in (\cap_{k' \in S_i} [V_{k'}]) \cap (\cap_{k' \in S_k} [V_{k'}])$, and then, $w \in [I_i] = \mathcal{N}(P_{J_i}^\perp)$. But this forces $P_{J_i}^\perp(w) = v$ and v to be zero and leads to vacuity.

(iii) $|\mathcal{J}_{i,l}| = 1$ and $|\mathcal{J}'_{i,l}| = 1$:

Suppose there is nonzero $v \in P_{J_i}^\perp(\cap_{k' \in S_k} [V_{k'}])$ with $k \in \mathcal{J}_{i,l}$. From Lemma 4, we have

$P_{I_l}^\perp(v) \in P_{I_l}^\perp(\cap_{k' \in S_k} [V_{k'}])$. By the same argument, $P_{I_l}^\perp(v) \in P_{I_l}^\perp(\cap_{k' \in S_i} [V_{k'}])$. Then

there is a nonzero $P_{I_l}^\perp(v) \in P_{I_l}^\perp(\cap_{k' \in S_i} [V_{k'}]) \cap P_{I_l}^\perp(\cap_{k' \in S_k} [V_{k'}])$.

(iv) $|\mathcal{J}_{i,l}| \geq 2$, $|\mathcal{J}'_{i,l}| = 0$ and $v \in P_{J_i}^\perp(\cap_{k' \in S_k} [V_{k'}])$ with some $k \in \mathcal{J}_{i,l}$: the same as case (ii).

(v) $|\mathcal{J}_{i,l}| \geq 2$, $|\mathcal{J}'_{i,l}| = 0$ and $v \notin P_{J_i}^\perp(\cap_{k' \in S_k} [V_{k'}])$ with any of $k \notin \mathcal{J}_{i,l}$:

We will show that this case is a generalization of case (ii) and also vacuous. As

$v \in +_{k \in \mathcal{J}_{i,l}} P_{J_i}^\perp(\cap_{k' \in S_k} [V_{k'}])$, we express

$$v = \sum_{j \in \mathcal{J}_{i,l}} a_j v_j$$

for each $a_j \in \mathbb{R}$ (at least two of them are nonzero) and $v_j \in P_{J_i}^\perp(\cap_{k' \in S_j} [V_{k'}])$.

By Lemma 5, for each v_j for $j \in \mathcal{J}_{i,l}$, we can find $S_{m,j}$ such that $v_j \in S_{m,j}$ and $m < i$, $m \neq j$, $S_m \cap S_i = \{0\}$. And this also implies that there exists certain $S_{t,j}$ and $v_j \in S_{t,j}$ such that $S_j \subset S_{t,j}$ and $S_{m,j} \subset S_{t,j}$. Here we point out that as $S_{t,j} \cap S_i \neq \emptyset$, since $S_j \cap S_i \neq \emptyset$. Then all $\cap_{k' \in S_{t,j}} [V_{k'}]$ for $j \in \mathcal{J}_{i,l}$ and their linear combinations are subsets of $[I_i]$. This leads to the conclusion $v \in [I_i]$ and shows the vacuity of this case.

(vi) $|\mathcal{J}_{i,l}| \geq 2$, $|\mathcal{J}'_{i,l}| \geq 1$ and $v \in P_{J_i}^\perp(\cap_{k' \in S_k} [V_{k'}])$ with some $k \in \mathcal{J}_{i,l}$:

If $k \in \mathcal{J}'_{i,l}$, then the same as the case (iii). If $k \notin \mathcal{J}'_{i,l}$, then the same as the case (ii).

(vii) $|\mathcal{J}_{i,l}| \geq 2$, $|\mathcal{J}'_{i,l}| \geq 1$ and $v \notin P_{J_i}^\perp(\cap_{k' \in S_k} [V_{k'}])$ with any of $k \in \mathcal{J}_{i,l}$:

As $v \in +_{k \in \mathcal{J}_{i,l}} P_{J_i}^\perp(\cap_{k' \in S_k} [V_{k'}])$, we express

$$v = \sum_{j \in \mathcal{J}_{i,l}} a_j v_j$$

for each $a_j \in \mathbb{R}$ (at least two of them are nonzero) and $v_j \in P_{J_i}^\perp(\cap_{k' \in S_j} [V_{k'}])$. Note that if $a_{j'} = 0$ for all $j' \in \mathcal{J}'_{i,l}$, then this case is essentially the same as case (v), so we only consider the situation at least one $a_{j'} \neq 0$ for $j' \in \mathcal{J}'_{i,l}$.

By Lemma 5 and its consequences in case (v), for each $j \in \mathcal{J}_{i,l} \setminus \mathcal{J}'_{i,l}$, there exists $S_{t,j}$ and $v_j \in S_{t,j}$ such that $S_j \subset S_{t,j}$ and $S_{m,j} \subset S_{t,j}$. As previously discussed, $\cap_{k' \in S_{t,j}} [V_{k'}]$ for $j \in \mathcal{J}_{i,l} \setminus \mathcal{J}'_{i,l}$ is a subset of $[I_i]$. So we rule out the terms involving $j \in \mathcal{J}_{i,l} \setminus \mathcal{J}'_{i,l}$ and then

$$P_{I_l}^\perp(v) = \sum_{j' \in \mathcal{J}'_{i,l}} a_{j'} P_{I_l}^\perp(v_{j'}).$$

Since each $\cap_{k' \in S_{j'}} [V_{k'}] \neq \{0\}$ for $j \in \mathcal{J}'_{i,l}$ is a subset of $[I_i]$ and at least one $a_{j'} \neq 0$, we deduce that $P_{I_l}^\perp(v)$ is non-zero. Therefore, the relative independence is violated.

□

Now the last term in the RHS of our law of nullity is re-expressed as

$$\begin{aligned} & (+_{k \in \mathcal{I}_{< i}} (\cap_{k' \in S_k} [V_{k'}])) \cap (\cap_{k \in S_i} [V_k]) \\ & = ((+_{k \in \mathcal{J}_{i,< l}} (\cap_{k' \in S_k} [V_{k'}])) \oplus (+_{k \in \mathcal{J}_{i,l}} P_{J_i}^\perp(\cap_{k' \in S_k} [V_{k'}]))) \cap (\cap_{k \in S_i} [V_k]) \\ & = ((+_{k \in \mathcal{J}_{i,< l}} (\cap_{k' \in S_k} [V_{k'}])) \oplus (+_{k \in \mathcal{J}_{i,l}} P_{J_i}^\perp(\cap_{k' \in S_k} [V_{k'}]))) \\ & \quad \cap (P_{J_i}(\cap_{k \in S_i} [V_k]) \oplus P_{J_i}^\perp(\cap_{k \in S_i} [V_k])) \end{aligned} \tag{9}$$

In Proposition 1, we have observed that $+_{k \in \mathcal{J}_{i,l}} P_{J_i}^\perp(\cap_{k' \in S_k} [V_{k'}])$ and $P_{J_i}^\perp(\cap_{k \in S_i} [V_k])$ are independent. As $P_{J_i}(\cap_{k \in S_i} [V_k]) \subset +_{k \in \mathcal{J}_{i,< l}} (\cap_{k' \in S_k} [V_{k'}])$, the term (9) becomes

$$(+_{k \in \mathcal{I}_{< i}} (\cap_{k' \in S_k} [V_{k'}])) \cap (\cap_{k \in S_i} [V_k]) = (+_{k \in \mathcal{J}_{i,< l}} (\cap_{k' \in S_k} [V_{k'}]) \cap (P_{J_i}(\cap_{k \in S_i} [V_k]))).$$

Finally, we have demonstrated

$$\begin{aligned}
\text{rank}([W_i]) &= \text{rank}(\cap_{k \in S_i} [V_k]) - \text{rank} \left(\left(+_{k \in \mathcal{I}'_{<i}} (\cap_{k' \in S_k} [V_{k'}]) \right) \cap (\cap_{k \in S_i} [V_k]) \right) \\
&= \text{rank}(\cap_{k \in S_i} [V_k]) \\
&\quad - \text{rank} \left(\left(+_{k \in \mathcal{J}_{i,<l}} (\cap_{k' \in S_k} [V_{k'}]) \right) \cap (P_{J_i}(\cap_{k \in S_i} [V_k])) \cap (\cap_{k \in S_i} [V_k]) \right) \\
&= \text{rank}(\cap_{k \in S_i} [V_k]) - \text{rank} (P_{J_i}(\cap_{k \in S_i} [V_k])) .
\end{aligned}$$

It is notable that the determination of $\text{rank}([W_i])$ depends only on $\mathcal{J}_{i,>l}$, that is, the set of indices j such that $|S_j| > |S_i|$ and $S_j \cap S_i \neq \emptyset$. In other words, it does not depend on any partial clusters of the same size as S_i and their orderings.

As principal score subspaces $[W_i]$ are constructed recursively and the determination of each $[W_i]$'s rank only depends on $\mathcal{J}_{i,>l}$, not on the ordering partial clusters of size $l = |S_i|$, we conclude that the set of pairs $\{(S_i, r(S_i)) : i \in \mathcal{I}\}$ is unique.

□

A.3 Proof of Theorem 2

Proof. We give a proof recursively on $l \in \mathcal{K}$. If $l = K$, there only exists $[W_1] = \cap_{k' \in S_1} [V_{k'}]$ for $S_1 = \mathcal{K}$, so there is nothing to prove. If $l = K - 1$, by absolute orthogonality, all $P_1^\perp(\cap_{k' \in S_i} [V_{k'}])$ are orthogonal each other for $i = \{2, \dots, K+1\}$. Therefore, in determining each $[W_i]$ for $i = \{2, \dots, K+1\}$, other $[W_t]$ for $t \in \mathcal{J}_{i,2} = \mathcal{I}_{<i} \cap \{i' : |S_{i'}| = 2\}$ does not affect on the construction of $[W_i]$.

For any $l \leq K - 2$, suppose the statement holds, that is, a principal score subspace $[W_j]$ such that $|S_j| = l' > l$ is uniquely determined only by $[W_{j'}]$ for $S_{j'} > S_j$. For each index $i \in \mathcal{J}_l = \{i' : |S_i| = l\}$ (regardless of ordering), we have $P_{I_l}(\cap_{k' \in S_i} [V_{k'}]) = P_{J_i}(\cap_{k' \in S_i} [V_{k'}])$ by absolute orthogonality. Then among all indices $i' \in \mathcal{J}_l$, $P_{J_{i'}}^\perp(\cap_{k' \in S_{i'}} [V_{k'}])$ are orthogonal each other.

Suppose an ordering on the set of all partial clusters of size l is given, denoted by

$(S_{i_1}, \dots, S_{i_h})$ with $h = {}_K C_l$. For i_1 , $[W_{i_1}]$ is just determined as $P_{J_{i_1}}^\perp(\cap_{k' \in S_{i_1}} [V_{k'}])$. Next for i_2 , as $[W_{i_1}]$ and $P_{J_{i_2}}^\perp(\cap_{k' \in S_{i_2}} [V_{k'}])$ are orthogonal, we check that $P_{i_1}^\perp \circ P_{J_{i_2}}^\perp(\cap_{k' \in S_{i_2}} [V_{k'}]) = P_{J_{i_2}}^\perp(\cap_{k' \in S_{i_2}} [V_{k'}])$. Thus $[W_{i_2}]$ is determined regardless of $[W_{i_1}]$. In recursive manner, for $i \in \{i_3, \dots, i_h\}$, $[W_i]$ is determined regardless of all $[W_{i'}]$ for $i' \in \mathcal{J}_{i,l}$, or in other word, is uniquely determined as $P_{J_i}^\perp(\cap_{k' \in S_i} [V_{k'}])$ depending only on $[W_{j'}]$ s for $S_{j'} > l$.

□

A.4 Proof of Corollary 1

Proof. From the discussions of Section 2, we know that $[W_{(k)}]$ is indeed the score subspace of Z_k for each $k = 1, \dots, K$. Thus, given unique $[W_i]$'s for $i \in \mathcal{I}_{(k)}$ from Theorem 2, the subspace $[U_{(k),i}]$ generated by $U_{(k),i}$ is unique. □

A.5 Examples

The following two examples presents the cases where relative independence is satisfied and not:

Example 4. Let $K = 3$, $n = 4$ and

$$V_1 = \begin{pmatrix} 1 & 0 \\ 0 & 1 \\ 0 & 0 \\ 0 & 0 \end{pmatrix}, \quad V_2 = \begin{pmatrix} 1 & 0 \\ 0 & 1/\sqrt{2} \\ 0 & 1/\sqrt{2} \\ 0 & 0 \end{pmatrix}, \quad V_3 = \begin{pmatrix} 1 & 0 \\ 0 & 0 \\ 0 & 1/\sqrt{2} \\ 0 & 1/\sqrt{2} \end{pmatrix}$$

then $[I_1] = [(1, 0, 0, 0)^T]$ and $P_{I_1}^\perp[V_1] = [(0, 1, 0, 0)^T]$, $P_{I_1}^\perp[V_2] = [(0, 1/\sqrt{2}, 1/\sqrt{2}, 0)^T]$ and $P_{I_1}^\perp[V_3] = [(0, 0, 1/\sqrt{2}, 1/\sqrt{2})^T]$ are linearly independent. Thus $\{[V_k]\}_{k \in \{1,2,3\}}$ is relatively independent.

Example 5. Let $K = 3$, $n = 4$ and

$$V_1 = \begin{pmatrix} 1 & 0 \\ 0 & 1 \\ 0 & 0 \\ 0 & 0 \end{pmatrix}, \quad V_2 = \begin{pmatrix} 1 & 0 \\ 0 & 1/\sqrt{2} \\ 0 & 1/\sqrt{2} \\ 0 & 0 \end{pmatrix}, \quad V_3 = \begin{pmatrix} 1 & 0 & 0 \\ 0 & 0 & 0 \\ 0 & 1 & 1/\sqrt{2} \\ 0 & 0 & 1/\sqrt{2} \end{pmatrix}$$

As $P_{I_1}^\perp[V_3] \cap (P_{I_1}^\perp[V_1] + P_{I_1}^\perp[V_2]) = [(0, 0, 1, 0)^T]$ is not empty, thus $\{[V_k]\}_{k \in \{1, 2, 3\}}$ is not relatively independent.

We present the following examples that support Theorem 1, that relative independence indeed guarantee the uniqueness of *partial clustering structure* $\mathfrak{S}_0 = \{(S_i, r(S_i)) : i \in \mathcal{I}, r(S_i) > 0\}$.

Example 6 (cont'd from Example 4.). Under the ordering $S_1 = \{1, 2, 3\}, S_5 = \{1\}, S_6 = \{2\}, S_7 = \{3\}$, we obtain $[W_1] = [(1, 0, 0, 0)^T], [W_5] = [(0, 1, 0, 0)^T], [W_6] = [(0, 0, 1, 0)^T]$ and $[W_7] = [(0, 0, 0, 1)^T]$. Then we have

$$\mathfrak{S}_0 = \{(\{1, 2, 3\}, 1), (\{1\}, 1), (\{2\}, 1), (\{3\}, 1)\}.$$

On the other hand, in the case $S_1 = \{1, 2, 3\}, S_5 = \{2\}, S_6 = \{1\}, S_7 = \{3\}$, we obtain $[W_1] = [(1, 0, 0, 0)^T], [W_5] = [(0, 1/\sqrt{2}, 1/\sqrt{2}, 0)^T], [W_6] = [(0, -1/\sqrt{2}, 1/\sqrt{2}, 0)^T]$ and $[W_7] = [(0, 0, 0, 1)^T]$. The partial clustering structure is still the same as above.

Example 7 (cont'd from Example 5.). Under the ordering $S_1 = \{1, 2, 3\}, S_5 = \{1\}, S_6 = \{2\}, S_7 = \{3\}$, we obtain $[W_1] = [(1, 0, 0, 0)^T], [W_5] = [(0, 1, 0, 0)^T], [W_6] = [(0, 0, 1, 0)^T]$ and $[W_7] = [(0, 0, 0, 1)^T]$. The partial clustering structure is

$$\mathfrak{S}_0 = \{(\{1, 2, 3\}, 1), (\{1\}, 1), (\{2\}, 1), (\{3\}, 1)\}.$$

On the other hand, in the case $S_1 = \{1, 2, 3\}, S_5 = \{3\}, S_6 = \{2\}, S_7 = \{1\}$, we obtain

$$[W_1] = [(1, 0, 0, 0)^T], [W_5] = [(0, 1, 0, 0)^T, (0, 0, 1/\sqrt{2}, 1/\sqrt{2})^T], [W_6] = [(0, 0, 1/\sqrt{2}, -1/\sqrt{2})^T]$$

and $[W_7] = \{0\}$. This time, the partial clustering structure is

$$\mathfrak{S}_0 = \{(\{1, 2, 3\}, 1), (\{1\}, 0), (\{2\}, 1), (\{3\}, 2)\}.$$

We also present the following examples that support Theorem 2, that absolute orthogonality guarantee the uniqueness of the principal score subspaces.

Example 8. Let $K = 4, n = 7$ and

$$\begin{aligned} V_1 &= \begin{pmatrix} 0 & 0 & 1 & 0 & 0 & 0 \end{pmatrix}^T \\ V_2 &= \begin{pmatrix} 0 & 0 & 0 & 1 & 0 & 0 \end{pmatrix}^T \\ V_3 &= \begin{pmatrix} 1/\sqrt{2} & 1/\sqrt{2} & 0 & 0 & 0 & 0 \\ 0 & 0 & 0 & 0 & 1 & 0 \end{pmatrix}^T \\ V_4 &= \begin{pmatrix} 1/\sqrt{2} & 1/\sqrt{2} & 0 & 0 & 0 & 0 \\ 0 & 0 & 0 & 0 & 0 & 1 \end{pmatrix}^T. \end{aligned}$$

This example satisfies absolute orthogonality. Between under two orderings ($S_{11} = \{3, 4\}, S_{12} = \{1\}, S_{13} = \{2\}$) and ($S_{11} = \{3, 4\}, S_{12} = \{2\}, S_{13} = \{1\}$), the determinations of $[W_{12}]$ and $[W_{13}]$ are the same.

Example 9. Let $K = 4$, $n = 7$ and

$$V_1 = \begin{pmatrix} 1/2\sqrt{2} & \sqrt{3}/2\sqrt{2} & 1/\sqrt{2} & 0 & 0 & 0 \end{pmatrix}^T$$

$$V_2 = \begin{pmatrix} \sqrt{3}/2\sqrt{2} & 1/2\sqrt{2} & 0 & 1/\sqrt{2} & 0 & 0 \end{pmatrix}^T$$

$$V_3 = \begin{pmatrix} 1/\sqrt{2} & 1/\sqrt{2} & 0 & 0 & 0 & 0 \\ 0 & 0 & 0 & 0 & 1 & 0 \end{pmatrix}^T$$

$$V_4 = \begin{pmatrix} 1/\sqrt{2} & 1/\sqrt{2} & 0 & 0 & 0 & 0 \\ 0 & 0 & 0 & 0 & 0 & 1 \end{pmatrix}^T.$$

This example satisfies relative orthogonality, but not absolute orthogonality. Between under two orderings ($S_{11} = \{3, 4\}$, $S_{12} = \{1\}$, $S_{13} = \{2\}$) and ($S_{11} = \{3, 4\}$, $S_{12} = \{2\}$, $S_{13} = \{1\}$), the determinations of $[W_{12}]$ and $[W_{13}]$ are not the same because $[V_1]$ and $[V_2]$ are not orthogonal and $[W_{11}] = (1/\sqrt{2}, 1/\sqrt{2}, 0, 0, 0, 0)^T$ does not have an effect on the determination of $[W_{12}]$ and $[W_{13}]$ by definition.

B Additional Information on Simulation Study

B.1 Example of Difference Measure between Two Partial Clustering Structures

For the comparison between two partial clustering structure, we devised a following concept of difference measure between partial clustering structures.

First, we introduce a *partial clustering structure matrix* \widehat{T} for a partial clustering structure $\widehat{\mathfrak{S}}_0$, a matrix each of whose columns indicates an identified partial cluster among datasets and each of whose elements show whether the corresponding dataset belongs to that partial cluster. For example, when $K = 3$, if the estimated partial clustering structure

is

$$\widehat{\mathfrak{S}}_0 = \{(\{1, 2, 3\}, 2), (\{1, 2\}, 1), (\{1, 3\}, 1), (\{2, 3\}, 1), (\{3\}, 1)\},$$

then

$$\widehat{T} = \begin{pmatrix} 1 & 1 & 1 & 1 & 0 & 0 \\ 1 & 1 & 1 & 0 & 1 & 0 \\ 1 & 1 & 0 & 1 & 1 & 1 \end{pmatrix}.$$

Next, consider two partial clustering structure matrices $\widehat{T}_1 \in \{0, 1\}^{n \times m_1}$ and $\widehat{T}_2 \in \{0, 1\}^{n \times m_2}$. Discarding all the identical columns between \widehat{T}_1 and \widehat{T}_2 , we denote the remaining columns \tilde{T}_1 and \tilde{T}_2 . For example, from

$$\widehat{T}_1 = \begin{bmatrix} 1 & 1 \\ 1 & 1 \\ 1 & 0 \end{bmatrix}, \quad \widehat{T}_2 = \begin{bmatrix} 1 & 1 & 0 \\ 1 & 1 & 1 \\ 1 & 1 & 1 \end{bmatrix},$$

we obtain

$$\tilde{T}_1 = \begin{bmatrix} 1 \\ 1 \\ 0 \end{bmatrix}, \quad \tilde{T}_2 = \begin{bmatrix} 1 & 0 \\ 1 & 1 \\ 1 & 1 \end{bmatrix}.$$

For each remaining column of \widehat{T}_1 (or \widehat{T}_2), find the closest column of \widehat{T}_2 (or \widehat{T}_1) in the Frobenius norm sense. The difference measure between \widehat{T}_1 and \widehat{T}_2 is the sum of the squares of all these Frobenius norms between the remaining columns between \tilde{T}_1 and \tilde{T}_2 . In the example above, for $(1, 1, 0)^T$ of \tilde{T}_1 , the closest column of \tilde{T}_2 is $(1, 1, 1)^T$ and the difference is 1. For $(1, 1, 1)^T$ of \tilde{T}_2 , the difference between $(1, 1, 0)^T$ is 1 and for $(0, 1, 1)^T$ of \tilde{T}_2 , it is 2. The overall difference between \widehat{T}_1 and \widehat{T}_2 is then $1^2 + 1^2 + 2^2 = 6$. The difference measure between two partial clustering structure matrix \widehat{T}_1 and \widehat{T}_2 is denoted $\text{diff}(\widehat{T}_1, \widehat{T}_2)$.

Finally, if the partial clustering structure $\widehat{\mathfrak{S}}_{0,1}$ (or $\widehat{\mathfrak{S}}_{0,2}$) has partial clustering structure matrices \widehat{T}_1 (or \widehat{T}_2), then the difference measure between $\widehat{\mathfrak{S}}_{0,1}$ and $\widehat{\mathfrak{S}}_{0,2}$ is $\text{diff}(\widehat{\mathfrak{S}}_{0,1}, \widehat{\mathfrak{S}}_{0,2}) = \text{diff}(\widehat{T}_1, \widehat{T}_2)$.

B.2 Review on Methodology of Other Methods

We briefly review the methodology of AJIVE (Feng et al., 2018), SLIDE (Gaynanova and Li, 2019), COBS (Gao et al., 2021) and JIVE (Lock et al., 2013).

AJIVE In AJIVE, each signal matrix $Z_k \in \mathbb{R}^{p_k \times n}$ is regarded as a sum of joint structure J_k and individual structure I_k for $k = 1, \dots, K$. A joint structure J_k is viewed as the score subspace $[V_M] \in \mathbb{R}^n$ shared by all Z_i 's.

AJIVE extracts each estimated signal matrix \widehat{Z}_k from dataset X_k and \widehat{Z}_k is of initial rank estimate \widetilde{r}_k . The estimated shared joint component $[\widehat{V}_M]$ is obtained as a flag mean among score subspaces of \widehat{Z}_k 's, or $[\widehat{V}_1], \dots, [\widehat{V}_k]$, in a sense of the projection Frobenius norm distance as our method. The rank r_J of $[\widehat{V}_M]$ (called the joint rank) is estimated using the simulated distribution of the largest singular value of the concatenated matrix of random directions and that of Wedin bounds:

- (1) If the largest squared singular value of the column concatenation matrix \widehat{V} of \widehat{V}_k 's is larger than the 5th percentile of the simulated distribution of the largest squared singular value of the concatenation matrix of random orthogonal matrices of the same size as \widehat{V}_k 's (or random direction bound), then $[\widehat{V}_M]$ is not generated by noise in 95 percent of probability.
- (2) If there are \widehat{r}_J squared singular values of \widehat{V} are larger than the 95th percentile of the simulated distribution of Wedin bounds, then the first \widehat{r}_J right singular vectors are used as the basis for the estimated joint score subspace $[\widehat{V}_M]$.

The estimated joint structure \widehat{J}_k is a projection of the dataset X_k onto the estimated joint score subspace $[\widehat{V}_M]$, that is, $\widehat{J}_k = X_k \widehat{V}_M \widehat{V}_M^T$. Each estimated individual structure \widehat{I}_k is obtained as $X_k \cdot (I - \widehat{V}_M \widehat{V}_M^T)$. The row spaces of each estimated individual structure \widehat{I}_k is orthogonal to $[\widehat{V}_M]$. There is no guarantee that individual structures are mutually orthogonal. The joint score matrix is just defined as \widehat{V}_M and the corresponding joint loading matrix for k th data source is a regression of \widehat{J}_k on \widehat{V}_M^T , computed as $\widehat{J}_k \cdot \widehat{V}_M$. The individual loading and score matrices are obtained from SVDs of \widehat{I}_k 's.

SLIDE SLIDE identifies the partial clustering structure with the penalized matrix factorization, that is,

$$(\widetilde{U}, \widetilde{V}) = \arg \min_{U, V} \sum_{k=1}^K \frac{1}{2} \|X_k - U_k V^T\|_F^2 + \lambda \sum_{j=1}^r \|U_{kj}\|_2 \quad \text{s.t. } V^T V = I,$$

where U_{kj} is the j th column of the loading matrix U_k of X_k and r is the number of all possible sparsity patterns. After computing \widetilde{U} and \widetilde{V} with an iterative algorithm, the corresponding structure matrix \widehat{T} is obtained from the sparse structure of \widetilde{U} . Note that the concept of the structure matrix \widehat{T} here is identical to the partial clustering structure matrix of ours in Section B.1. Even though this optimization problem is nonconvex and there is no guarantee about convergence to the global optimum, authors reported that a local solution can be obtained heuristically by initializing V with the left singular matrix of concatenated X that works well in the simulation.

Then SLIDE estimate the loading and score matrices, \widehat{U} and \widehat{V} , for the structure \widehat{T} by solving the following optimization problem with an iterative algorithm,

$$(\widehat{U}, \widehat{V}) = \arg \min_{U, V} \|X - UV^T\|_F^2 \quad \text{s.t. } V^T V = I,$$

with the constraint that the loading U has the same sparsity structure as \widehat{T} .

In model validation, SLIDE adapt the block cross validation (BCV) procedure to select the best structure $\widehat{T}_{\text{best}}$. BCV splits rows and columns of each dataset X_k into submatrices

$X_k^{11}, X_k^{12}, \dots, X_k^{21}, \dots$. Then it holds out a set of submatrices $X^{ij} = [X_1^{ij}, X_2^{ij}, \dots, X_K^{ij}]$ of the same sub-block position in each dataset X_k and evaluate the prediction error on X^{ij} 's. Given a set of structure candidates $\widehat{T}_1, \widehat{T}_2, \dots$, we select one that minimizes the error across all folds.

JIVE Like in AJIVE, JIVE decompose each signal matrix X_i as a sum of joint structure J_i and individual structure I_i , for $i = 1, \dots, K$. After defining R to be a row concatenation of $R_i = X_i - J_i - I_i$, JIVE estimate both joint and individual structures by minimizing $\|R\|_F^2$ under the given ranks. An alternating iterative algorithm is implemented for the estimation finding individual component with given joint component at one step and vice versa at another step. The estimated joint structure is identical to the first r_J terms in the SVD of X with individual components removed and the estimated individual structures to the first r_i terms in the SVD of X_i with the joint component removed. The selection of r_J and r_i s are validated using the permutation test.

COBS COBS iteratively estimates a sequence of loading vectors, u_i for $i = 1, \dots, r$ for given r , while updating the data matrix $X = [X_1, \dots, X_k] \in \mathbb{R}^{n \times \sum p_k}$. The algorithm starts with $X^{[0]} = X$. At the i th step, with the current data matrix $X^{[i-1]}$, the i th loading vector u_i is estimated solving the following maximization problem, that is,

$$\tilde{u}_i = \max_u \|(X^{[i-1]})^T u\|_2^2 \quad \text{s.t. } u^T u = 1.$$

As each u_i is equipped with block structure $u_i = (u_{(1)}^T \dots u_{(K)}^T)^T$, we can give sparsity at two levels of thresholding, one for block-wise sparsity and the other for overall sparsity in estimating \tilde{u}_i . The tuning parameters $\alpha_v \in [0, 1]$ and $\lambda_v \geq 0$ control the two levels of sparsity respectively, and \hat{u} is thresholded as a normalized solution of

$$\min_x \frac{1}{2} \|x - \tilde{u}_i\|^2 + \gamma_1 \|x\|_1 + \gamma_2 \|x\|_{2,1},$$

where $\gamma_1 = \alpha_v \lambda_v$ and $\gamma_2 = (1 - \alpha_v) \lambda_v$. Then the score vector v_i is estimated as the empirical BLUP and dataset $X^{[i-1]}$ is updated as $X^{[i]} = X^{[i-1]} - \hat{u}_i \hat{v}^T$.

B.3 Additional Simulation Results

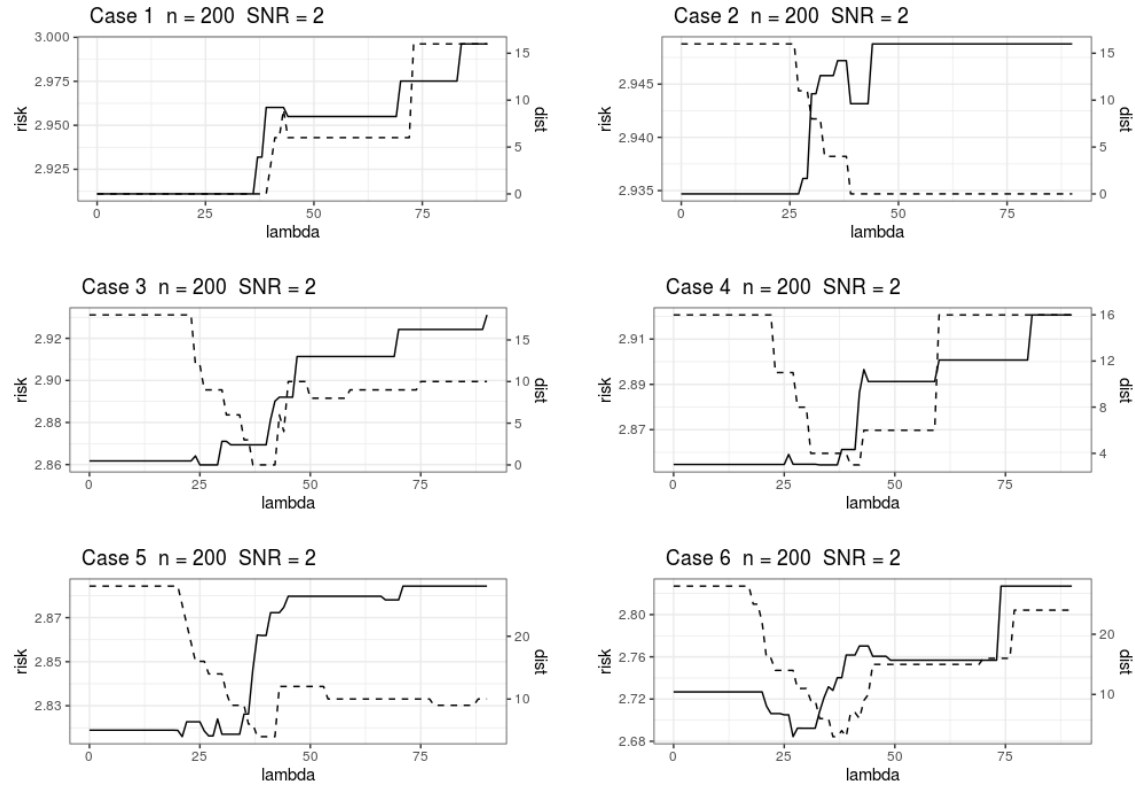


Figure 6: The values of penalized empirical risk for λ when $n = 200$ and SNR = 2.

Table 5: Time comparison among our method and other four method(SLIDE, COBS, AJIVE and JIVE). The computation time reported. The unit is second(s). Averages and standard deviations are over 10 replications

Model	SNR	PSI-MDI	SLIDE bcr	COBS	AJIVE	JIVE
1	10	0.88 (0.13)	2.66 (0.1)	10.05 (0.05)	11.43 (0.02)	5.71 (0.05)
	5	0.79 (0.00)	3.41 (0.14)	10.97 (0.06)	11.44 (0.02)	5.72 (0.04)
2	10	1.01 (0.21)	1.05 (0.03)	4.39 (0.05)	11.44 (0.02)	21.82 (6.68)
	5	0.93 (0.01)	0.87 (0.03)	3.85 (0.04)	11.45 (0.01)	20.52 (4.74)
3	10	1.72 (0.15)	3.58 (0.08)	10.6 (0.05)	11.23 (0.02)	58.33 (19.05)
	5	1.5 (0.01)	4.87 (0.16)	10.45 (0.06)	11.23 (0.04)	34.83 (0.02)
4	10	1.5 (0.14)	4.36 (0.16)	14.47 (0.04)	11.28 (0.06)	26.28 (13.47)
	5	1.23 (0.07)	5.91 (0.24)	14.1 (0.05)	11.26 (0.02)	33.27 (22.91)
5	10	2.48 (0.13)	5.73 (0.19)	13.45 (0.06)	11.1 (0.04)	61.81 (30.06)
	5	1.91 (0.06)	8.87 (0.23)	13.15 (0.05)	11.31 (0.42)	36.43 (6.58)
6	10	2.88 (0.13)	10.75 (0.31)	24.14 (0.07)	11.08 (0.21)	22.58 (0.04)
	5	2.01 (0.07)	22.82 (0.72)	27.61 (0.05)	10.99 (0.02)	43.93 (8.81)

B.4 Simulation Settings for Section 5.4

In the unbalance of signal strength between joint and individual component settings, we set $n = 200$ and $K = 3$.

In the first case, we set the elements of σ_M^2 as

- (1) Joint (S_1) : $(15, 14.5, \dots, 5.5)$,
- (2) Individual 1 (S_2) : $(0.150, 0.141, 0.132, \dots, 0.069)$,
- (3) Individual 2 (S_3) : $(0.147, 0.138, 0.129, \dots, 0.066)$,
- (4) Individual 3 (S_4) : $(0.144, 0.135, 0.126, \dots, 0.063)$,

so the strength of joint signals are about 100 times stronger than those of individual signals.

In the second case, we set the elements of σ_M^2 as

- (1) Joint (S_1) : $(0.15, 0.145, \dots, 0.055)$,
- (2) Individual 1 (S_2) : $(15, 14.1, 13.2, \dots, 6.9)$,
- (3) Individual 2 (S_3) : $(14.7, 13.8, 12.9, \dots, 6.6)$,
- (4) Individual 3 (S_4) : $(14.4, 13.5, 12.6, \dots, 6.3)$,

so the strength of individual signals are about 100 times stronger than those of joint signals.

C Additional Information on Real Data Analysis

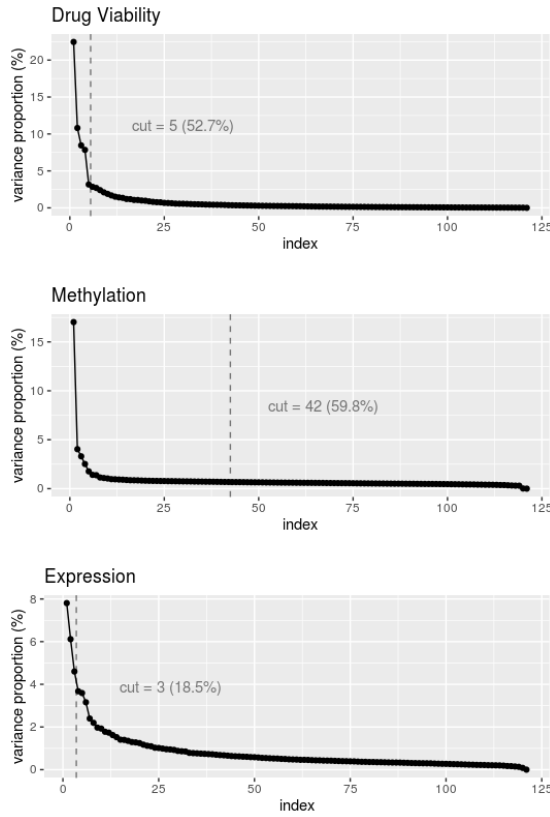


Figure 7: The scree plots for Drug, Meth and Exp datasets. The ranks $r_1 = 5$, $r_2 = 42$ and $r_3 = 3$ explain 60.8%, 60.4%, 68.4% of variation for Drug, Meth and Exp datasets.

Table 6: Fisher's exact tests between gene mutations/chromosome defects and the CLL subgroups, α and β were conducted simultaneously. The p-values were adjusted with the FDR (Benjamini-Hochberg method) and the top 5 lowest FDR (BH method) adjusted p-values were listed.

Gene mutation/Chromosome defect	adjusted p-value
IGHV	1.036×10^{-13}
MED12	0.173
del17p13	0.174
del13q14	0.178
TP53	0.184

Table 7: The association between IGHV mutation status and the CLL subgroups with an FDR (BH method) adjusted p-value **1.036×10^{-13}** from the Fisher's exact test. Nine missing data for IGHV mutation status were excluded.

Mutation \ Subgroup	α	β
IGHV Wild type	49	8
IGHV Mutated	7	48

Table 8: The most appeared drugs in the subgroups [a] and [b] with appearances at least four times out of 5 concentrations.

The most appeared drugs in subgroup [a]		
Drug name	Target pathway	Appearances
spebrutinib	BTK	5
idelalisib	PI3K delta	5
duvelisib	PI3K gamma, PI3K delta	5
tamatinib	SYK	5
dasatinib	ABL1, KIT, LYN, PDGFRA, PDGFRB, SRC	5
PF 477736	CHK1, CHK2	5
MK-2206	AKT1/2 (PKB)	5
ibrutinib	BTK	4
selumetinib	MEK1/2	4
PRT062607 HCL	SYK	4
AZD7762	CHK1/2	4
CCT241533	CHK2	4
TAE684	ALK	4
MK-1775	WEE1	4
AT13387	HSP90	4

The most appeared drugs in the subgroup [b]		
Drug name	Target pathway	Appearances
everolimus	mTOR	5
thapsigargin	SERCA	5
orlistat	LPL	5
rotenone	Electron transport chain in mitochondria	5
afatinib	EGFR, ERBB2	4
fludarabine	Purine analogue	4
navitoclax	BCL2, BCL-XL, BCL-W	4

References

Asendorf, N. A. (2015). *Informative data fusion: Beyond canonical correlation analysis*. Ph. D. thesis, University of Michigan.

Bai, J. and S. Ng (2002). Determining the number of factors in approximate factor models. *Econometrika* 70(1), 191–221.

Björck, A. and G. Golub (1973). Numerical methods for computing angles between linear subspaces. *Mathematics of Computation* 27(123), 579–594.

Dietrich, S., M. Oleś, J. Lu, L. Sellner, and et al. (2018). Drug-perturbation-based stratification of blood cancer. *Journal of Clinical Investigation* 128(1), 427–445.

Draper, B., M. Kirvy, J. Marks, T. Marrinan, and C. Peterson (2014). A flag representation for finite collections of subspaces of mixed dimensions. *Linear Algebra and its Applications* 451, 15–32.

Eckart, C. and G. Young (1936). The approximation of one matrix by another of lower rank. *Psychometrika* 1, 211–218.

Feng, Q., M. Jiang, J. Hannig, and J. Marron (2018). Angle-based joint and individual variation explained. *Journal of Multivariate Analysis*, 241–265.

Gao, X., S. Lee, and S. Jung (2021). Covariate-driven factorization by thresholding for multi-block data. *Biometrics* 77(3), 1011–1023.

Gaynanova, I. and G. Li (2019). Structural learning and integrative decomposition of multi-view data. *Biometrics* 75, 1121–1132.

Horst, P. (1961a). Generalized canonical correlations and their applications to experimental

data. *Journal of Clinical Psychology* 72(2), 331 – 347.

Horst, P. (1961b). Relations among sets of measures. *Psychometrika* 26(2), 129 – 149.

Hotelling, H. (1936). Relations between two sets of variates. *Biometrika* 28(3/4), 321–377.

Kettenring, J. R. (1971). Canonical analysis of several sets of variables. *Biometrika* 58, 433–451.

Li, G. and I. Gaynanova (2018). A general framework for association analysis of heterogeneous data. *The Annals of Applied Statistics* 12(3), 1700–1726.

Li, G. and S. Jung (2017). Incorporating covariates into integrated factor analysis of multi-view data. *Biometrics* 72, 1433–1442.

Lock, E., K. Hoadley, J. Marron, and A. Nobel (2013). Joint and individual variation explained (jive) for integrated analysis of multiple data types. *Annals of Application Statistics* 7(1), 523–542.

Meredith, W. (1964). Rotation to achieve factorial invariance. *Psychometrika* 29(2), 187 – 206.

Mshaik, R., J. Simonet, A. Georgievski, and et al. (2021). Hsp90 inhibitor nvp-bep800 affects stability of src kinases and growth of t-cell and b-cell acute lymphoblastic leukemias. *Blood Cancer Journal* 11(61).

Nielsen, A. A. (1994). *Analysis of Regularly and Irregularly Sampled Spatial, Multivariate, and Multi-temporal Data*. Ph. D. thesis, Institute of Mathematical Modelling / Technical University of Denmark, Lyngby, Denmark.

Norris, J. L., M. A. Farrow, D. B. Gutierrez, et al. (2017). Integrated, high-throughput, multiomics platform enables data-driven construction of cellular responses and reveals global drug mechanisms of action. *Journal of Proteome Research* 16(3), 1364–1375.

Reuter, J. A., D. Spacek, and M. P. Snyder (2015). High-throughput sequencing technologies. *Molecular Cell* 58(4), 586–597.

St.Thomas, B., L. Lin, L.-H. Lim, and S. Mukherjee (2014). Learning subspaces of different dimensions. arXiv:1404.6841.

Subramanian, I., S. Verma, S. Kumar, A. Jere, and K. Anamika (2020). Multi-omics data integration, interpretation, and its application. *Bioinformatics and Biology Insights*.

Vershynin, R. (2018). *High-dimensional Probability* (1 ed.). Cambridge University Press.

Vinograde, B. (1950). Canonical positive definite matrices under internal linear transformations. *Proceedings of American Mathematical Society* 1, 159–161.

Wang, C. and R. J. Youle (2014). The role of mitochondria in apoptosis. *Annu Rev Genet.* 43, 95–118.

Ye, K. and L.-H. Lim (2016). Schubert varieties and distances between subspaces of different dimensions. *SIAM Journal of Matrix Analysis and Applications* 37(3), 1176–1197.

Zhang, Y. and T. Hunter (2014). Roles of chk1 in cell biology and cancer therapy. *International Journal of Cancer* 134(5), 1013–1023.